Texas Medical Center Library
DigitalCommons@TMC

UT GSBS Dissertations and Theses (Open Access)　　　　Graduate School of Biomedical Sciences

8-2018

Development and Commissioning of an Independent Peer Review System for a Small Animal Irradiator

Mary Peters

Follow this and additional works at: https://digitalcommons.library.tmc.edu/utgsbs_dissertations

Part of the Oncology Commons, and the Physics Commons

The TMC LIBRARY
Health Sciences Resource Center

DEVELOPMENT AND COMMISSIONING OF AN INDEPENDENT PEER REVIEW

SYSTEM FOR A SMALL ANIMAL IRRADIATOR

By

Mary Elizabeth Peters, B.S.

APPROVED:

_____
Rebecca M Howell, Ph.D.
Advisory Professor

_____
David S Followill, Ph.D.

_____
Sunil Krishnan, M.D.

_____
Stephen F Kry, Ph.D.

_____
Mohammad R Salehpour, Ph.D.

_____
Ramesh C Tailor, Ph.D.

_____

APPROVED:

_____
Dean, The University of Texas
MD Anderson Cancer Center UT Health Graduate School of Biomedical Sciences

DEVELOPMENT AND COMMISSIONING OF AN INDEPENDENT PEER REVIEW

SYSTEM FOR A SMALL ANIMAL IRRADIATOR

A

THESIS

Presented to the Faculty of

The University of Texas

MD Anderson Cancer Center UTHealth

Graduate School of Biomedical Sciences

in Partial Fulfillment

of the Requirements

for the Degree of

MASTER OF SCIENCE

by

Mary Elizabeth Peters, B.S.

Houston, Texas

August 2018

Dedication

To my parents, Dan and Patty Peters, for their endless love, support, and encouragement. Thank you for inspiring me to follow my heart and passion and for devoting your lives to providing me with opportunities for success.

Acknowledgements

First and foremost, I would like to acknowledge my research advisor for this project, Dr. Rebecca Howell. Thank you for recognizing my potential and always pushing me to become a better researcher and medical physicist.

Thank you to my committee members: Drs. Ramesh Tailor, David Followill, Stephen Kry, Sunil Krishnan, and Mohammad Salehpour. I greatly appreciate your input in this project and your commitment to my success and professional development.

Special thank you to Susan Smith, for sharing with me your knowledge of thermoluminescent dosimetry, John Costales, for creating my phantoms, and Francisco Aguirre, Paola Alvarez, and Dr. Joshua Niedzielski, for assisting me with measurements. Thank you, Dr. Daniel Craft, for always assisting me with my research projects and serving as a role model.

Thank you, Dr. Richard Wendt, for your dedication to students and this program. I cannot express enough gratitude to you for all you have done for me. Thank you, Frances Quintana, for being a constant source of joy.

I would like to express my sincerest gratitude to Dr. Mohammad Salehpour. Thank you for encouraging me to pursue my PhD and for always having my best interest at heart.

Thank you, Dr. Julianne Pollard-Larkin, for your mentorship. Your energy and enthusiasm are contagious.

Lastly, a huge thank you to my family. Thank you to my parents, Patty and Dan Peters, for being my biggest supporters and encouraging me to pursue my

dreams, no matter the distance between us. Thank you to my brother, Jeffery

Peters, for reminding me the importance of having fun in this short lifetime. Thank

you to my fiancé, Joel Gronberg, for believing in me and supporting me in this

journey. Lastly, thank you to the Etheredges and the Gronbergs for welcoming me

with open arms into your families and making Texas feel like home.

Abstract

DEVELOPMENT AND COMMISSIONING OF AN INDEPENDENT PEER REVIEW

SYSTEM FOR A SMALL ANIMAL IRRADIATOR

Mary Elizabeth Peters, B.S.

Advisory Professor: Rebecca M Howell, Ph.D.

Dosimetry for small animal irradiators lacks the standardization of clinical radiotherapy practice, yet plays a central translational role in human trial design. The purpose of this work was to improve the dosimetric accuracy and consistency of animal studies by developing an independent peer review system to verify dose delivery from animal irradiators. This study focused on the development of a mouse phantom and characterization of the thermoluminescent dosimetry system for a commonly used small animal irradiator.

First, a mouse model and irradiation stand were designed with the purpose of being used in a mailable audit. Two mouse phantoms were machined from high impact polystyrene; one accommodated three thermoluminescent dosimeters (TLD) and the other an Exradin A1SL 0.053 cc ion chamber (Standard Imaging, Middleton, WI) for cross-comparison with the TLD. An acrylic irradiation stand was constructed to allow users to align the mouse phantom to the irradiator's isocenter. Second, the mouse system was commissioned in a small animal irradiator using a 225 kVp beam. A pseudo tissue-air ratio was determined using the ion chamber mouse phantom. The dose rate was determined using the TG-61 "in-air" method, along

with the measured half-value layer of the beam. The response of the TLD in the mouse phantom was characterized under identical irradiation conditions. Lastly, the commissioned mouse system was mailed to two institutions to verify feasibility of the service.

We designed a robust, user-friendly mouse phantom and foldable irradiation stand, ideal for a mail audit service. The system was commissioned at 225 kVp in a small animal irradiator.   The energy correction factor for TLD in the mouse phantom was 0.792 (SD=0.006) relative to ^{60}Co. This factor can be applied to validate dose delivered in this model of animal irradiator. The feasibility of the independent peer review system was demonstrated by verifying beam output and small animal dosimetry for two institutions.

We established and commissioned a methodology for independent peer review of mouse dosimetry for a commonly used animal irradiator. This methodology can be used to characterize other commercially available orthovoltage irradiators.

Table of Contents

List of Illustrations

List of Tables

Chapter 1: Introduction and Background

Background to the Problem

The results from pre-clinical research, i.e., animal studies, are used to assist in the design of clinical trials for human subjects. Accurate and reproducible pre-clinical radiation biology research is essential for designing meaningful clinical trials in radiation oncology that will advance cancer treatments. As described in a recent review article, the National Cancer Institute (NCI) is concerned with the lack of success of recent clinical trials (Zakeri, Coleman, & Vikram, 2018). The article analyzed results of recent prospective randomized trials in radiation oncology for clinical significance. Notably and of concern, approximately half of the clinical trials were not proven to be clinically significant, highlighting the need for improved clinical trial design, which starts with improved pre-clinical research.

A recent NCI U01 funding opportunity announcement had explicit instructions requiring accurate and reproducible dosimetry for the testing of targeted agents administered with radiation therapy and chemotherapy in cell and animal studies (National Institutes of Health, 2016). The program announcement emphasized the importance of robust pre-clinical studies in order to improve the potential success of human trials. In order for pre-clinical work to be robust, standardization is needed. This need was emphasized in the program announcement, which explicitly stated, "In radiation studies, as in other preclinical testing, there is a need for standardization of assays, for the development of improved models, as well as a framework for cross-validation of pre-clinical results." The program announcement addressed specific action items for improving standardization, including stating the "precise targeting,

timing, and dosing of radiation" and "ensuring accuracy and consistency of irradiation protocols through [National Institute of Standards and Technology (NIST)]-traceable dosimetry testing and ongoing validation, and detailed, translatable reporting of irradiation set-up details."   Not only does the announcement state specific methodology, but a mandatory component of the modular budget was the inclusion of a minimum of fifty thousand dollars towards NIST-traceable dosimetry. This is the first time that such explicit details regarding radiation dosimetry and standardization have been specifically defined in an NCI program announcement for molecularly targeted therapy in animals and cells. This paradigm shift toward including mechanisms to ensure accurate radiation dosimetry in pre-clinical studies suggests that the NCI is concerned that failures in recent clinical trials are related to the lack of accurate and consistent dosimetry in those studies.

Several studies have investigated the need for improved dosimetry reporting in pre-clinical studies in order to improve the translation of preclinical research into the clinic. One report investigated preclinical studies for ten popular radiation dose enhancers (Stone et al., 2016). The report evaluated 125 preclinical studies, 104 in vitro and 51 in vivo. The studies' methods were evaluated for clarity. A subset of the methods analyzed was reporting of radiation parameters, including: radiation source type, energy, dose rate, setup, and equipment calibration. The percentages of in vitro and in vivo papers for which these radiation parameters were clearly reported are summarized in Table 1. The lack of reporting of irradiation parameters is concerning for several reasons. First, it makes it impossible for other researchers to reproduce the experiment and compare experimental results. Second, lack of reporting makes it unclear whether the dosimetry within the studies was accurate. The report's review

highlights these two key concerns, stating, "with deficiencies in reporting dosimetry and irradiation setup, it was not possible to know whether researchers had accounted for such factors as dose from backscatter, uniformity of dose across the radiation field or through the depth of the tumor, absorption by overlying culture medium, culture vessel or tissues, and whether dosimetry had been carried out under the same conditions as the experimental setup or was traceable to equipment calibrated by NIST. Lack of this information makes it impossible to replicate the studies and to compare results within and among laboratories." The results of pre-clinical research on very complex radiation biology mechanisms have no meaning if the dosimetry is incorrect and others cannot reproduce the results. This is of particular concern for radiation threshold experiments, where the absorbed dose associated with a radiation-induced effect is being reported, e.g., erythema onset (Desrosiers et al., 2013).

Radiation Parameter	Studies that Reported the Specified Parameter (%)	
	In Vitro Studies	In Vivo Studies

Source	86	80
Energy	81	63
Dose rate	62	57
Setup	24	55
Equipment Calibration	8	20

Table 1. Reporting of radiation parameters in a survey of one hundred and twenty-five preclinical studies[1]

Concerns regarding standardization in animal studies led the NCI, the National Institute of Allergy and infectious Diseases (NIAID), and NIST to host a workshop on Radiation Dosimetry Standardization in Radiobiology in September 2011 (Desrosiers et al., 2013). There were two major goals of this workshop. The first was to highlight the need for dosimetry standardization, and the second was to discuss the necessary efforts for improving standardization in the future. Workshop participants put forth a list of recommendations for improving standardization. Key takeaways from these recommendations were the need for collaboration among biologists and physicists, the need for dosimetry comparison programs, and suggestions for the dosimetry content that should be included in radiobiology publications. In regards to the latter takeaway, participants proposed four categories of dosimetry information be mandated for publication of pre-clinical trial data for

---

[1] Table 1 is compiled from:
Stone Helen B, Bernhard Eric J, Coleman C Norman, Deye James, Capala Jacek, Mitchell James B, Brown J Martin. Preclinical data on efficacy of 10 drug-radiation combinations: Evaluations, concerns, and recommendations. *Transl Oncol.* 2016;9(1):46-56. doi:10.1016/j.tranon.2016.01.002

studies involving radiation therapy: (1) absolute dosimetry and beam calibration (2) methodology for determination of absorbed dose within research subjects, (3) specification of the radiation source, and (4) irradiation details.

A major discussion topic at the 2011 workshop was the need for dosimetry comparison programs, i.e., independent peer review, specifically for radiation biology. Independent peer review for dosimetry is well established for megavoltage (MV) linear accelerators. For MV linear accelerators, independent peer review is available from several different agencies/groups including the International Atomic Energy Agency (IAEA) (Izewska, Bera, & Vatnitsky, 2002); European Organization for Research and Treatment of Cancer (EORTC) (Hurkmans et al., 2016); Australian Clinical Dosimetry Service Radiotherapy Trials Quality (ACDS) (Williams et al., 2012); Japan Clinical Oncology Group (JCOG) (Okamoto et al., 2018); Radiotherapy Clinical Trials: Quality Assurance Group (RTTQA) (Clark et al., 2015); University of Wisconsin Radiation Monitoring by Mail (UWRMM), (Yegingil et al., 2012;"Radiation Monitoring by Mail Services," n.d.); MD Anderson Radiation Dosimetry Services (RDS) (Aguirre et al., 2003); and Imaging and Radiation Oncology Core (IROC) Houston QA Center (Aguirre et al., 2003;Ibbott, 2010). However, there is no parallel service offered for small animal irradiators. The University of Wisconsin Accredited Dosimetry Calibration Laboratory (UWADCL) has assisted with a couple of small pilot mail audits of beam outputs for small animal irradiators. One study by Seed *et al.* found that only four out of seven institutions were able to deliver doses within five percent of the prescribed dose for their radiation biology setups (Seed et al., 2016). The second study by Pedersen *et al.* tested twelve beams at ten different institutions, and found that only five out of the twelve were within five percent accuracy (Pedersen et al.,

2016). Furthermore, six out of the twelve beams were outside of a ten percent accuracy criterion. These studies demonstrate a clear need for a widely available independent peer review system for small animal irradiators used for radiobiological pre-clinical studies.

The market for small animal irradiators has recently shifted from the use of isotope source irradiators to X-ray orthovoltage irradiators. However, this shift in technology has not been accompanied by new procedures or any formal recommendations regarding calibration of such units. Orthovoltage beam calibration recommendations were defined by the American Association of Physicists in Medicine (AAPM) Task Group 61 (TG-61) (Ma, 2001). However, TG-61 was published more than 15 years ago (2001) before current orthovoltage "cabinet" irradiators were widely used. There are many challenges related to applying TG-61 protocol within the confines of cabinet irradiator geometries as opposed to the clinical external beam orthovoltage radiotherapy units for which the protocol was developed. The lack of calibration protocols for this specific new technology reinforces the importance of the workshop recommendations for the involvement of a physicist in the design and implementation of radiation biology research and the need for dosimetry comparison programs. In the University of Wisconsin Accredited Dosimetry Calibration Laboratory mail audit studies referenced above, several of the institutions tested were operating orthovoltage small animal irradiators. In the study by Seed *et al.*, three of the labs were operating x-ray irradiators (Seed et al., 2016). Only one of the three labs passed. One of the two failing labs had dose errors as large as forty-two percent. None of the orthovoltage labs had physicists on staff, and two out of the three were reliant on manufacturer's specifications for dosimetry. In the study by Petersen *et al.*, five out

of the twelve facilities were x-ray facilities. Only one of these five x-ray facilities passed. The average deviation between the measured and intended dose was seventeen percent.

Orthovoltage Small Animal Irradiators

The need for dedicated precision irradiators for pre-clinical research and the subsequent onset of orthovoltage small animal irradiators is best described in a review article by Verhaegen *et al.,* detailed below (Verhaegen, Granton, & Tryggestad, 2011).

The past twenty years have seen major advancements in radiation therapy. Modern treatments utilize beam modulation and image-guidance, resulting in improved tumor control and reduced normal tissue complications. These technological advancements in radiation therapy were not immediately matched by subsequent advancements in radiobiology research. Therefore, modern treatments were adapted without validation in animal models. However, in the past decade, several research groups developed dedicated precision small animal irradiators that make it possible to mimic modern radiotherapy in small animals (Verhaegen et al., 2011).

In order to mimic human responses using small animals, both the radiation beam size and energy needed to be appropriately scaled. Treating small animals using clinical megavoltage (MV) photon beams is not appropriate and does not resemble human treatments, although this methodology was used to derive much of the available clinical guidelines on tumor control probability and normal tissue complication probability. MV beams result in dose build-up/down gradients at tissue

interfaces due to electronic disequilibrium. The scale of these gradients is on the order of the size of small animals, making it impossible to deliver a uniform dose to the tumor in a mouse using megavoltage energies. Most of the dedicated precision small animal irradiators that are being widely used today contain an x-ray source, although some use radioactive sources (Verhaegen et al., 2011). The dominance of orthovoltage irradiators over active source irradiators for pre-clinical research is likely attributed to several factors, including: the ability to select a desired treatment energy from a wide range of energies, the strict regulations associated with operating an active source irradiator, and the need to replace radioactive sources due to decay. Verhaegen *et al.* describes the advantages of using orthovoltage energies to treat small animals. Unlike MV photon beams, orthovoltage beams experience minimal dose buildup effects at material interfaces, making them ideal for treating small animals. Another advantage of orthovoltage beams is their sharp radial dose profile, reducing the dose delivered to surrounding normal tissues. This advantage is critical in small animals given the small size of the target and close proximity of normal structures (Verhaegen et al., 2011).

State of the art orthovoltage small animal irradiators are commercially available from Precision X-Ray (North Branford, CT) and Xstrahl Medical & Life Sciences (Camberley, Surrey) (Butterworth, Prise, & Verhaegen, 2015). Precision X-Ray's most advanced irradiator on the market is the X-RAD Small Animal Radiotherapy (SmART) unit (Figure 1), the successor of the X-RAD 225Cx. The major competitor for the X-RAD SmART is the Xstrahl Small Animal Radiation Research Platform (SAARP) (Figure 2). Both irradiators achieve sub-millimeter targeting accuracy, an important requirement given that entire anatomical structures

in mice and rats are on the order of centimeters. The single x-ray tube in these irradiators is used for both imaging and therapy via interchangeable filter packs, enabling image-guided treatments. They are capable of fast (approximately one minute) precision imaging via cone beam computed tomography (CBCT) by either rotating the x-ray source and detectors or rotating the animal. Both of these systems also offer bioluminescent optical imaging (Verhaegen et al., 2011). Researchers can inject Luciferase, a light emitting enzyme, into small animals in order to visualize tumor or disease (Sadikot, 2005). The optical photons are detected using charge-coupled device (CCD) cameras. Incorporating fast, functional imaging capabilities into small animal research platforms is commendable. Bioluminescent optical imaging has enabled researchers to assess treatment response and study adaptive radiation therapy. However, researchers should be aware of the limitations of bioluminescent optical imaging in regards to signal localization. Positron emission tomography (PET) scans have far superior localization due to coincidence detection. Previously acquired PET scans and scans from other modalities can be fused with bioluminescent optical imaging and CBCT images. The precision on-boarding imaging, along with the ability to fuse previously acquired Digital Imaging and Communications in Medicine (DICOM) images from other modalities, enable targeting accuracies on the order of 100-200 μm (Verhaegen et al., 2011; "X-RAD SmART Small Animal Image Guided Irradiation System," n.d.).

Figure 1. Precision X-Ray's X-RAD Small Animal Radiotherapy (SmART) unit[2]

Figure 2. Xstrahl's Small Animal Radiation Research Platform (SAARP)[3]

Butterworth *et al.* reports on the capabilities of current small animal image-guided radiotherapy devices. Both Precision X-Ray and Xstrahl provide research platforms that can plan and deliver clinically relevant treatments that align with

---

[3] Figure 2 adapted from: https://xstrahl.com/life-science-systems/muriplan/. Accessed June 7, 2018.

Phase 1 clinical trials. Precision X-Ray offers a treatment planning software called SmART-Plan, developed at MAASTRO clinic (Maastricht, Netherlands). SmART-Plan computes dose using CBCT images and Monte Carlo simulations. Xstrahl's treatment planning software is called Muriplan. It utilizes graphical processing units (GPUs) to compute dose based on advanced superposition convolution algorithms (Butterworth et al., 2015). Both platforms are capable of planning and treating using static beams or complex arcs. Non-coplanar therapy is also possible, as both the SmART and SARRP units have rotating animal platforms. Both companies offer motorized collimators, enabling intensity modulated radiation therapy (IMRT). The SARRP unit is capable of respiratory gating combined with temperature and heart rate monitoring ("X-RAD SmART Small Animal Image Guided Irradiation System," n.d.; "Small Animal Radiation Research Platform," n.d.).

While precision orthovoltage small animal irradiators are transforming translational radiobiology, they lack many of the capabilities of modern MV linear accelerators. Small animal irradiators are not equipped with multi-leaf collimators. Furthermore, inverse treatment planning and automated contouring are not yet available. Of greatest concern, quality assurance guidelines and methodologies for small animal irradiators are lacking. Without processes and procedures for testing dosimetric accuracy and reproducibility, experimental results can't be verified.

Thermoluminescent Dosimetry

Thermoluminescent dosimeters (TLD) are solid state, integrating passive dosimeters (Attix, 1986; Khan & Gibbons, 2014). They are commonly used in clinical practice for skin dose measurements, brachytherapy dose-rate constant

measurements (Nunn et al., 2008), and of particular relevance to our work, independent peer review. TLD are both practical and appropriate for independent peer review because of their small size, high dosimetric accuracy, and their ability to "hold" dose for readout at a later time.

The American Association of Physicists in Medicine (AAPM) Task Group 191 (TG-191) report provides recommendations to the medical physics community on the appropriate use of luminescent dosimeters in a clinical setting. It details the theory of TLD, phosphor crystals containing small impurities (Kry et al., n.d.). These imperfections are utilized to measure dose. When energy in the form of ionizing radiation is deposited in TLD, charges are excited and can become trapped in the crystal impurities. During readout, these trapped charges are released by stimulating the crystal with heat, resulting in the emission of visible light. Resulting luminescence is detected with a photomultiplier tube (PMT). Finally, correction factors are applied to relate the energy collected to the dose delivered to the TLD (Kry et al., n.d.).

TLD signal can be converted to dose using a calibration factor defined for a user's specific irradiation and readout conditions. It is typically defined using TLD standards, or TLD irradiated to a known dose under specific irradiation conditions in reference energy beam. TLD standards are then used to determine the calibration factor, also referred to as the sensitivity, for each reading session. This factor directly relates signal to dose under standard conditions. As in TG-51 methodology, the dose under experimental conditions is calculated using a series of correction factors relating the experimental conditions to the TLD standards conditions (Almond, Biggs, & Hanson, 1999). The following equation is used:

$$D = M_{corr} N k_F k_L k_Q k_\theta,$$

where M_{corr} is the corrected reading collected during the TLD readout process, N is

the system calibration coefficient referred to above, k_F is the fading correction factor,

k_L is the linearity correction factor, k_Q is the beam quality correction factor, and k_θ is

the angular correction factor. The details of each term in the equation are discussed

further below (Kry et al., n.d.).

For TLD powder, the mass of the powder needs to be accounted for since the

amount of powder is directly related to the luminescence. The corrected reading is

reported as signal per unit mass. The reading may be corrected for background

signal by reading a TLD that has not been irradiated. The system calibration

coefficient, N, is often defined for each reading session by reading TLD standards.

The calibration coefficient for the reading session is determined by dividing the dose

delivered to the standards by the corrected reading (Kry et al., n.d.).

Each of the "k" correction factors relates the experimental conditions to the

standards conditions since the calibration coefficient is only valid for the irradiation

and reading conditions of the standards. The exponential decay of the TLD signal

with time is referred to as fading. Fading can be explained by the spontaneous

release of electrons occupying shallow traps at room temperature. A large amount

of the TLD signal is lost in the first 24 hours after irradiation. Fading stabilizes after

a couple days, when the majority of the low energy traps have emptied. Because of

the exponential decay fading relationship, TLD are usually read about a week after

irradiation, when the signal has stabilized. The fading correction factor, k_F, is

needed if the time between irradiation and reading for the experimental TLD is

different than that of the standards. This correction factor, as well as the other correction factors, are commissioned for each batch of TLD. A batch of TLD is a group created from the same crystal. Once the correction factors for the batch are determined, they can be assumed to be uniform (Kry et al., n.d.).

The linearity correction factor, k_L, refers to the varying sensitivity of signal with the dose delivered. There is a linear response between dose and signal at low energies (up to 4 or 5 Gy). However, the response becomes supralinear and eventually flat as the dose is increased. This relationship is measured and plotted during batch commissioning. The linearity correction factor corrects for the differences in sensitivity for the dose delivered to the experimental TLDs versus the standards (Kry et al., n.d.).

The energy correction factor, k_Q, accounts for the change in TLD sensitivity with beam quality. Of particular relevance to this study, TLD over respond at low energies (in the orthovoltage range) relative to megavoltage energies.   Thus, when TLD are used to measured dose in orthovoltage irradiators, it is critical to fully and accurate characterize k_Q. There are two components of the energy correction factor, presented by the TG-191 committee: an intrinsic energy dependence and a medium-dependent energy dependence. The intrinsic energy dependence is the change in signal per dose to the detector versus energy. It accounts for how radiation interacts with the crystal at different energies, *i.e.*, the different trapping and recombination mechanisms in the phosphor crystal that occur at different energies. The medium-dependent energy dependence accounts for the fact that the TLD material is used to determine dose to a material of interest (usually tissue, water, or muscle). The relationship between the dose delivered to TLD and the dose delivered to

surrounding tissue changes with energy as a result of differences in mass attenuation coefficients and stopping-power ratios (Kry et al., n.d.). The large over-response of TLD by up to 40% in the diagnostic range is primarily a result of this phenomenon. The photoelectric effect is the dominating radiation interaction mechanism at low energies. Its probability is related to the third power of the atomic number (Z^3) (Khan & Gibbons, 2014). The most commonly used TLD material, TLD-100, is composed of lithium fluoride (LiF). LiF has an atomic number of 8.3, as compared to 7.2 for soft tissue (Scarboro et al., 2011). Therefore, the probability of the photoelectric effect in LiF is 1.53 times that in soft tissue. The energy correction factor is not separated into its two components when measured. An overall energy correction factor corrects for the differences in TLD sensitivity for the experimental versus standards beam quality.

Lastly, the angular correction factor is needed if the orientation of the incident radiation on the experimental TLD is different from that of the standards. However, because the TLD capsules used in this study are cylindrically symmetric, an angular correction factor is not needed.

Radiation Dosimetry Services (RDS) Independent Peer Review

MD Anderson RDS is one of several organizations around the world that offers independent peer review in the form of mail audits. Mail audits play a major role in improving the quality of radiation therapy centers. RDS offers several independent peer review services including: beam output checks for external radiation therapy machines, dose verification for total body and total skin procedures, and dose verification for blood irradiators used by blood banks

("Radiation Dosimetry Services: Mailed Thermoluminescent Dosimeters (TLD) for Quality Assurance," n.d.). Orthovoltage irradiators are among the external radiation therapy machines that RDS offers beam output checks for. Orthovoltage output is checked by irradiating TLD capsules on top of an irradiation stand. With the increased use of small animal irradiators in the past several years, RDS has received beam output check requests for these dedicated pre-clinical cabinet irradiators. Over the past five years, RDS has been monitoring beam output of X-RAD irradiators from several institutions with a passing criterion of $\pm10\%$. Independent peer review of beam output ensures that cabinet irradiators are properly calibrated. However, RDS does not currently have the ability to check small animal dosimetry. Developing and commissioning a mouse phantom for independent peer review in small animal irradiators would enable RDS to more thoroughly test the dosimetry of pre-clinical studies.

Statement of the Problem

In the past decade, dedicated precision animal irradiators have become widely available. Today, they are commonly used for pre-clinical research. The results from radiation biology studies are used to design clinical trials. However, the accuracy and reproducibility of pre-clinical research is lacking. There is no widely available service for independent peer review for small animal irradiators. Small scale preliminary studies suggest that approximately 65-80% of institutions operating orthovoltage irradiations have large dosimetric inaccuracies (Pedersen et al., 2016; Seed et al., 2016). The availability of independent peer review for small animal irradiators would improve dosimetric standardization in radiation biology

experiments, leading to improved success of clinical trials and advancements in modern radiotherapy.

Project Objective

The overall objective of this project was to develop and commission an independent peer review system for small animal irradiators. In particular, we focused on a commonly used animal irradiator, the X-RAD 225Cx (Precision X-Ray, North Branford, CT). Once developed, this methodology can be further expanded to include other types of commercially available irradiators.

Hypothesis

An independent peer review system for a small animal irradiator can be developed that has a total (1-sigma) uncertainty of less than ±10%.

Specific Aims

The four specific aims below were designed to test the hypothesis.

1. To design a mouse phantom that is appropriate for a mailable peer review TLD audit service.
2. To characterize the half value layer of the animal irradiator, and to determine dose in the animal irradiator using an ion chamber and following AAPM TG-61 protocol.
3. To characterize the energy correction factor for TLD in the mouse phantom in the small animal irradiator.
4. To conduct a feasibility study of the developed audit service by sending the phantoms to at least two sites to verify the output of their irradiators.

Chapter 2: Development of the Independent Peer Review Service

Mouse Phantom Design

Methods

3D Printed Mouse Phantom

The first approach to creating a mouse phantom was to utilize 3D printing technology. A computed tomography (CT) scan of an average sized laboratory mouse was obtained from a radiation biology laboratory at our institution. OsiriX (Bernex, Switzerland) software was used to import the CT scan and create a 3D model of the mouse. The mouse model was edited using MeshLab software (Pisa, Italy) to remove the nose cone used to anesthetize the mouse. The unedited and edited versions of the mouse model are shown in Figures 3a and 3b, respectively. Simplify3D software (Cincinnati, Ohio) was then used to convert the model into a printable file. The mouse phantom was printed in two pieces using NinjaFlex material on a commercial 3D printer.
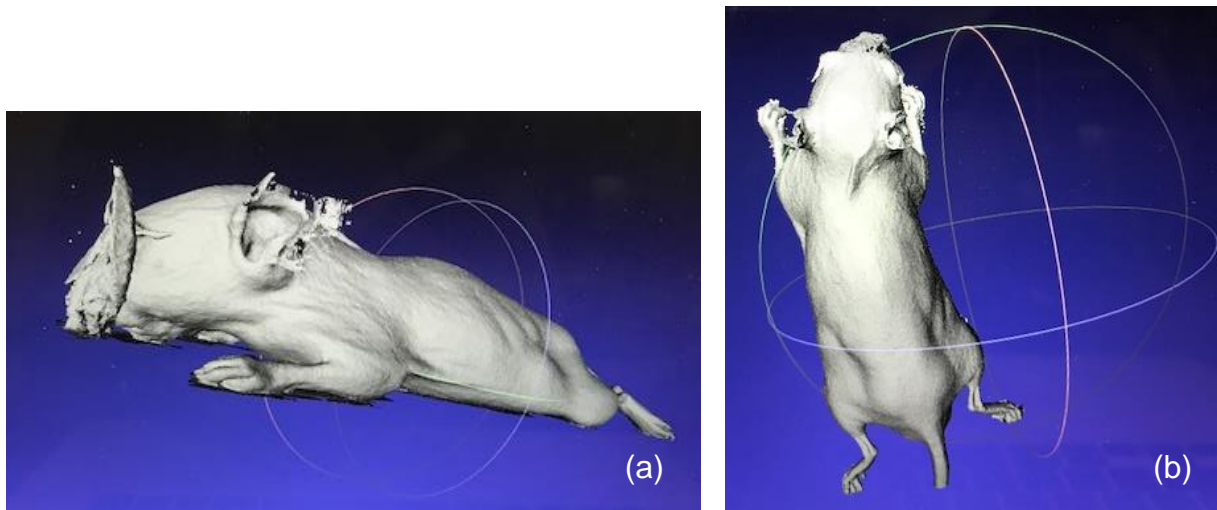
Figure 3. Unedited (a) and edited (b) mouse model in MeshLab

Machined Mouse Phantom

Based on preliminary results (see section 3D Printed Mouse Phantom below), we determined that a 3D printed phantom was not sufficiently robust for a mailable audit system and chose to move forward with a stylized, machined phantom made of high impact polystyrene (HIPS). Such phantoms have been well characterized by the MD Anderson RDS, which has used stylized HIPS for ten years for its peer review service of orthovoltage energy blood irradiators.

We aimed to develop a mouse phantom with dimensions similar to a typical mouse used in radiation biology experiments. Thus, we measured the dimensions of five C57BL/6J strain mice (3 male and 2 female) at 8, 10, and 12 weeks of age. The following measurements were taken: whole-body length (from the tip of the nose to the start of the tail), head length, head depth, head width, chest length, chest depth, chest width, flank depth, and tail length. The measurements are shown in Table 2.

Age	id	whole body length (mm)	head length (mm)	head depth (mm)	head width (mm)	chest length (mm)	chest depth (mm)	chest width (mm)	flank depth (mm)	tail length (mm)
8 weeks	m1	87.5	27.5	12.0	15.3	29.7	15.2	19.7	13.5	65.6
	m2	83.9	27.0	11.6	14.7	27.8	13.8	20.0	12.2	67.3
	m3	85.6	27.5	11.9	15.9	19.2	14.6	19.1	11.5	69.1
		85.7	27.3	11.8	15.3	25.6	14.5	19.6	12.4	67.3
	f1	80.5	27.2	13.4	14.7	26.1	17.5	19.7	13.2	65.3
	f2	82.1	28.1	11.7	17.5	27.7	15.1	19.1	12.1	69.2
		81.3	27.7	12.6	16.1	26.9	16.3	19.4	12.7	67.3
10 weeks	m1	90.7	26.8	12.2	15.9	31.6	15.1	23.4	13.0	70.5
	m2	90.4	28.0	12.1	15.2	26.1	15.3	23.5	15.3	68.6
	m3	87.6	26.8	14.1	15.2	27.7	15.2	22.6	13.0	71.6
		89.6	27.2	12.8	15.4	28.5	15.2	23.2	13.8	70.2
	f1	85.3	26.3	13.0	16.4	26.2	14.2	23.2	12.2	70.8
	f2	88.3	26.2	12.0	15.0	26.6	16.8	21.4	14.6	74.7
		86.8	26.3	12.5	15.7	26.4	15.5	22.3	13.4	72.8
12 weeks	m1	94.8	28.7	12.8	15.2	26.4	17.0	25.0	14.4	89.7
	m2	88.9	29.1	12.0	16.3	16.3	14.9	24.1	14.1	70.2
	m3	89.9	28.9	13.7	17.0	25.4	17.1	26.2	12.7	70.7
		91.2	28.9	12.8	16.2	22.7	16.3	25.1	13.7	76.9
	f1	84.2	26.5	10.8	13.8	24.3	15.5	20.4	12.8	67.0
	f2	85.3	27.4	12.4	15.0	25.3	14.1	22.7	13.2	70.4
		84.8	27.0	11.6	14.4	24.8	14.8	21.6	13.0	68.7

Table 2. Measured mouse dimensions[4]

The average measurements were used to determine appropriate dimensions for the symmetric mouse phantom. The shape of the mouse was simplified using a partial cylinder of diameter 25 mm to represent the body and a cone to represent the head. The height of the phantom was 20 mm, and the length was 85 mm. The basic dimensions of the phantom are shown in Figure 4. The lengths of the phantom

---

[4] *male and female mice indicated with id that begins with m or f, respectively*

body and head are illustrated in Figure 4a. The height and width of the phantom are

shown (as viewed from the backside) in Figure 4b.
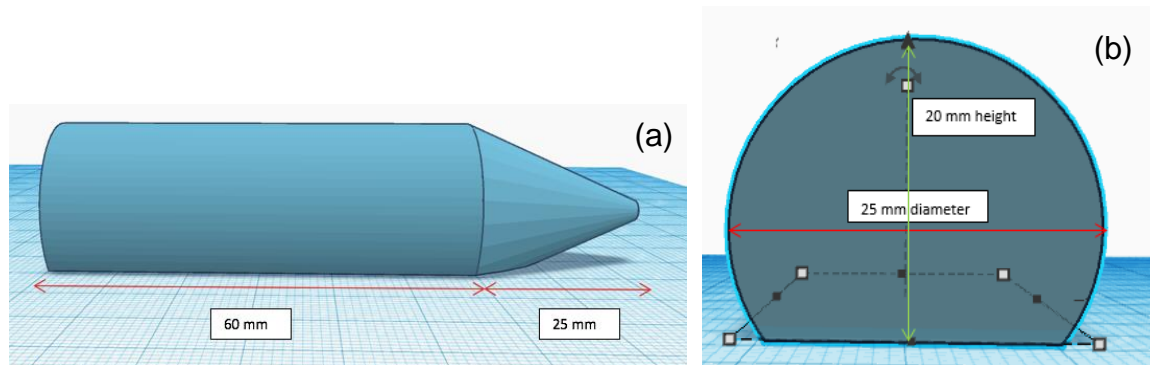
Figure 4. High impact polystyrene mouse phantom dimensions

Results

3D Printed Mouse Phantom

The NinjaFlex 3D printed mouse phantom is shown in Figure 5. The

approach of 3D printing the phantom was not further pursued due to two key

limitations. First, a key aspect of mailable audits is that the phantoms be robust in

terms of mechanical integrity because they will undergo thousands of shipments and

irradiations. The soft 3D printed phantom material, along with the small size of the

extremities were not sufficiently robust. Second, the energy dependence of the

material must be well defined for beam energies in which it will be irradiated. While

the 3D printed material had been characterized for megavoltage photon and electron

beams (Craft et al., 2018), it had not been characterized in orthovoltage beams.
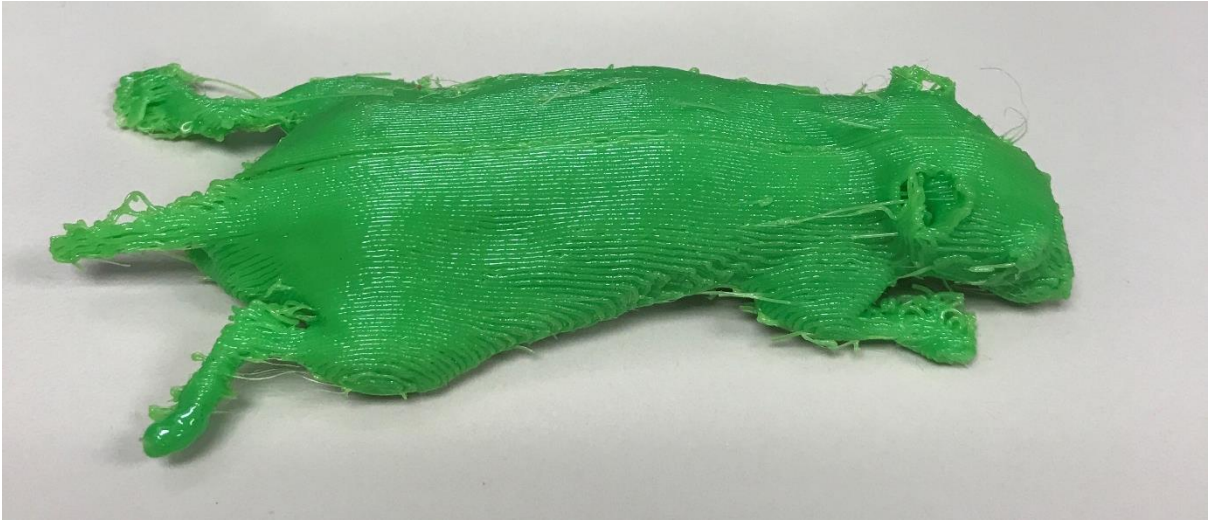
Figure 5. 3D printed mouse phantom

Machined Mouse Phantom

Two mouse phantoms were machined from HIPS; one accommodated three thermoluminescent dosimeters (TLD) and the other an Exradin A1SL 0.053 cc ion chamber (Standard Imaging, Middleton, WI) for cross-comparison with the TLD. The phantoms were designed so that the centroid of the ion chamber is at the same location as the center of the TLD powder in the middle TLD capsule. The model of the mouse phantom that was designed to accommodate TLD and an ion chamber are shown in Figure 6a and 6b, respectively.

(a) (b)
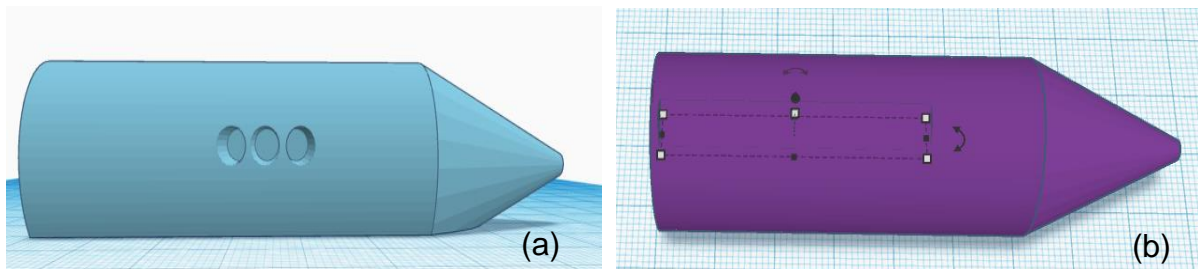
Figure 6. Model of high impact polystyrene thermoluminescent dosimeter (a) and ion chamber (b) mouse phantoms

The machined mouse phantoms constructed of HIPS are robust and user friendly, ideal for a mail audit service. Both the TLD and ion chamber phantoms, shown in Figure 7a and 7b, respectively, contain crosshairs for alignment with the irradiator's isocenter using the unit's wall lasers. The TLD phantom was constructed to ensure a snug fit for the TLD capsules and to allow easy loading and unloading of the capsules between irradiations. Holes of very small diameter behind the TLD capsule holes enable the capsules to be unloaded with the tip of a paperclip.

(a) (b)
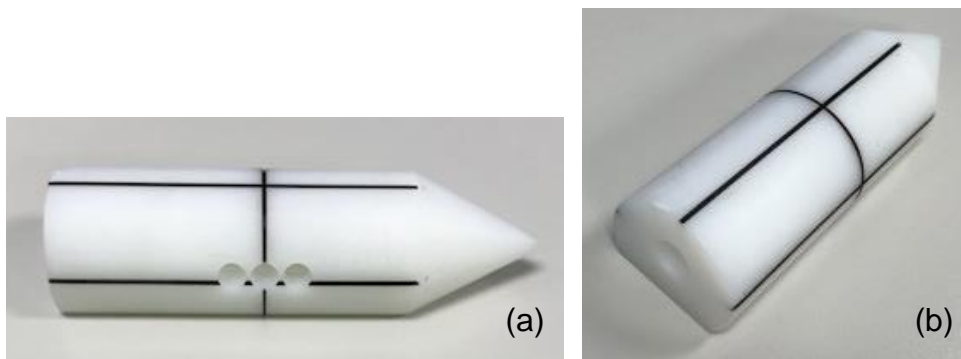
Figure 7. High impact polystyrene thermoluminescent dosimeter (a) and ion chamber (b) mouse phantoms

Irradiation Stand Design

Methods

An irradiation stand was designed to ensure a reproducible set-up for the mail audit service. Note that in this investigation, we focused on designing a stand for the X-RAD 225Cx small animal irradiator. However, an analogous method could be followed to design irradiation stands for other manufacturers and models. A box shaped irradiation stand was designed to allow users to align the mouse phantom to the irradiator's isocenter. Acrylic was selected as the material for the stand because it has a low scatter cross section and is translucent, ensuring optimal visibility during

setup. A foldable design was chosen to reduce shipping costs for the service. The height of the stand needed to be such that the center of the mouse phantom would align with the beam isocenter. To determine the appropriate stand height, we therefore measured the distance from the metal plate at the base of the irradiator to the isocenter.

Results

A foldable irradiation stand was created as a platform for the developed mouse phantom. The foldable irradiation stand was constructed out of sheets of Lexan 0.16 cm thick. The stand is easily assembled using tape (Figure 8). The distance from the metal plate at the base of the irradiator to the isocenter at our institution was measured to be 28.8 cm. However, the variation in isocenter distance for different units, even of the same model, has not been characterized. Thus, to accommodate for possible variation in this distance, we designed a stand with a nominal height of 26 cm, to which the user can add sheets of acrylic or paper to achieve the appropriate height in their unit. A stand width of 15 cm was selected because it does not interfere with the 10 cm by 10 cm irradiation field. The platform that sits on top of the stand is 18 cm by 18 cm. The developed irradiation stand ensures reproducibility in the irradiation setup for independent peer review.

Figure 8. Assembled irradiation stand

Chapter 3: Commissioning the Independent Peer Review System

Determination of True Dose in the Animal Irradiator

Methods

Measuring Beam Output for Small Animal Irradiator

Mechanical Isocenter Check

Because beam output is determined at the irradiator's isocenter, a mechanical isocenter check was performed prior to taking any output measurements. An in-house isocenter position indicator (pointer) was inserted into the accessory tray that was used for this test. As the source tube was rotated through 360 degrees, coincidence of the lasers with the tip of the isocenter pointer was checked. Agreement within 1 mm between the lasers and isocenter pointer throughout the gantry rotation indicated that the mechanical isocenter is correctly located. Figure 9 illustrates the coincidence of the laser intersection with the isocenter pointer when the gantry is positioned so that the beam axis is vertically downwards.
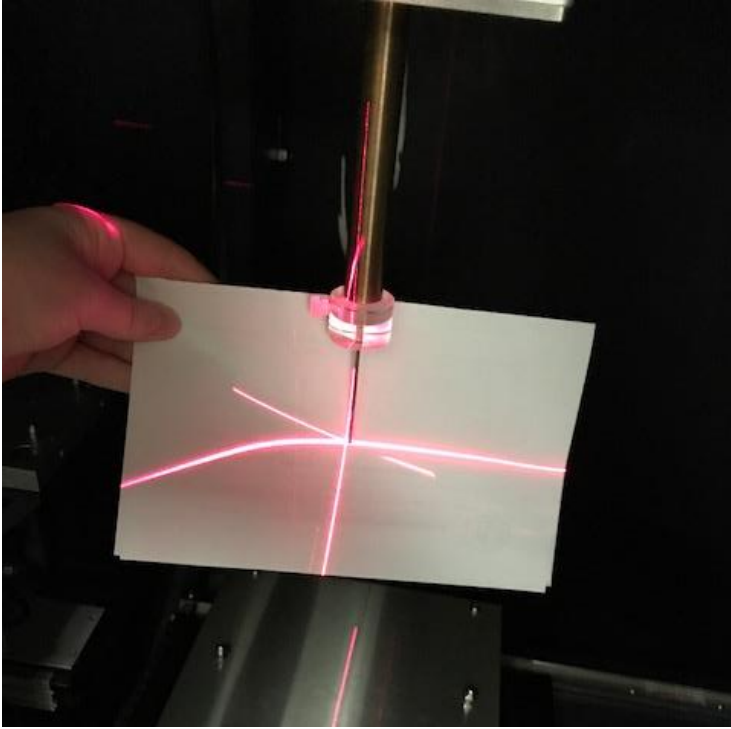
Figure 9. Mechanical isocenter check

Half-Value Layer Measurements

Application of the TG-61 protocol requires accurate measurement of half-value layer (HVL) under narrow-beam geometry (Ma, 2001). An in-house narrow-beam collimator was designed (by R. Tailor) to achieve true narrow-beam geometry in the small animal irradiator. The collimating device consists of two Cerrobend plates of 1.6 mm thickness, separated by a vertical distance of 3.3 cm, with a 1.0 cm diameter aperture. The removable collimator (Figure 10) was designed to be placed on top of a Styrofoam stand (Figure 11), which houses the attenuating material and the ion chamber (Exradin A1SL) according to good geometric conditions, reducing the amount of scattered radiation reaching the detector. The narrow-beam half-value

layer for the X-RAD 225Cx was measured using copper and aluminum sheets for the maximum beam quality, 225 kVp and 13 mA, over the course of several months.
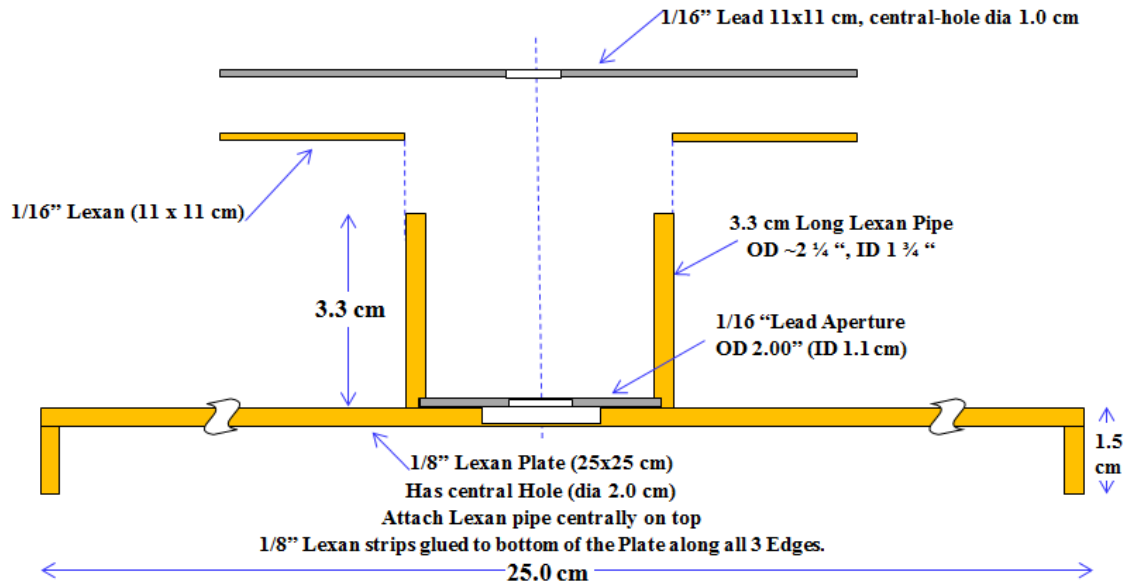
Figure 10. Schematic diagram of the narrow-beam collimator
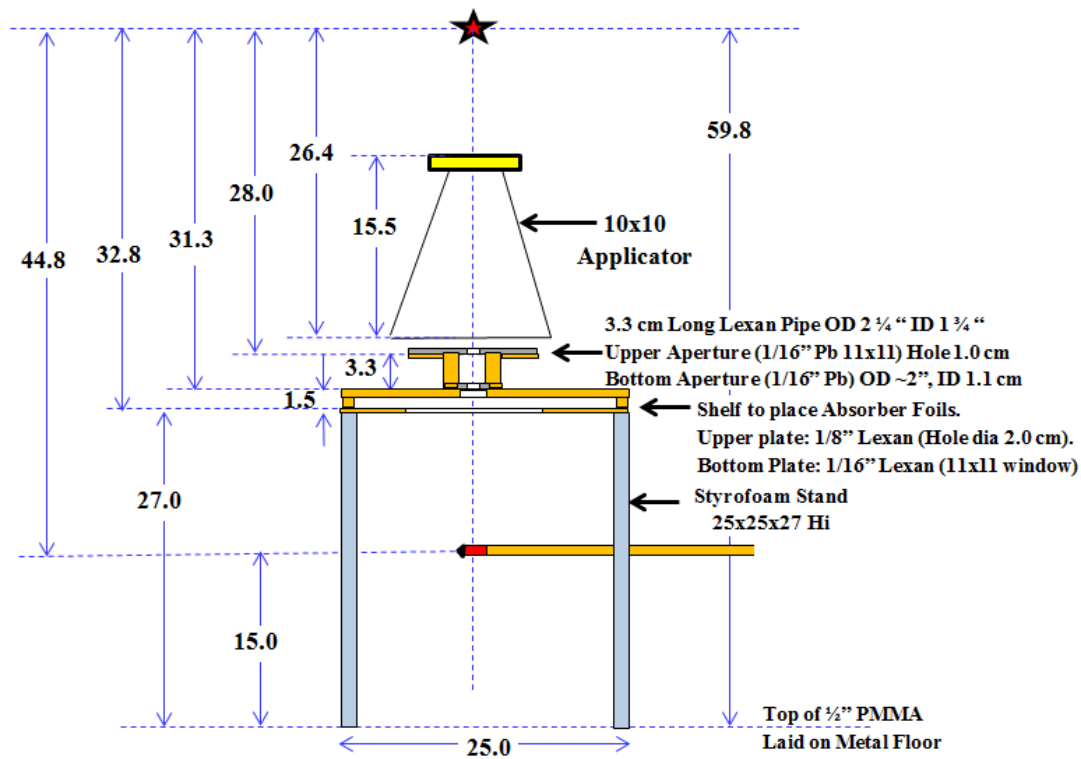
Figure 11. Schematic diagram of the narrow-beam collimator on top of the

Styrofoam stand[5]

Air-kerma Calibration and TG-61 In-Air Method

Reference dosimetry of clinical orthovoltage irradiators is described in the

AAPM TG-61 protocol (Ma, 2001). The TG-61 report contains two dosimetry

methods, "in-air" and "in-phantom". Both methodologies are based on an air-kerma

standard, with measurements performed with an ionization chamber that has been

calibrated in air in terms of air-kerma at a standards laboratory. The in-phantom

method determines absorbed dose to water at 2 cm depth within a water phantom

that is at least 30 x 30 x 30 cm^3. We used the in-air methodology to calibrate the X-

---

[5] Dimensions are in centimeters unless stated otherwise

RAD 225Cx at our institution because its inner dimensions could not accommodate an appropriately sized phantom. Specifically, we measured dose at a reference point in air to determine absorbed dose to water at the surface of a water phantom.

The A1SL ion chamber used for determining TG-61 beam output was calibrated for air-kerma at the University of Wisconsin ADCL. An air-kerma calibration factor relates the corrected ion chamber reading to the air-kerma, as shown in Equation 1:

$$\text{Equation 1: } N_K = \frac{K_{air}}{M}$$

where N_K is the air-kerma calibration factor for a given beam quality, K_{air} is the air-kerma at the reference point, and M is the corrected ion chamber reading at the reference point (Ma, 2001). Our A1SL ion chamber was calibrated for four different tungsten anode orthovoltage beam qualities, listed in Table 3. Air-kerma calibration factor was plotted as a function of HVL for the four beam qualities (Figure 12). The air-kerma calibration factor for the X-RAD 225Cx was selected from the fitted curve (Figure 12) for the unit's measured HVL.

Beam Quality	Added filter (mm Al or Cu)	HVL1 (mm Al)	HVL1 (mm Cu)	Air Kerma Rate (mGy/sec)	Air Kerma Calibration Coefficient (Gy/C)	Exposure Calibration Coefficient (R/C)
UW200-M	1.00 Al + 1.01 Cu	14.8	1.63	1.930	5.375×10^8	6.136×10^{10}
UW120-M	3.0 Al + 0.10 Cu	6.77		2.365	5.355×10^8	6.113×10^{10}
UW80-M	2.75 Al	3.00		1.821	5.453×10^8	6.225×10^{10}
UW-60M	1.50 Al	1.65		1.796	5.615×10^8	6.410×10^{10}

Table 3. Air-kerma calibration coefficients measured at the University of Wisconsin Accredited Dosimetry Calibration Laboratory
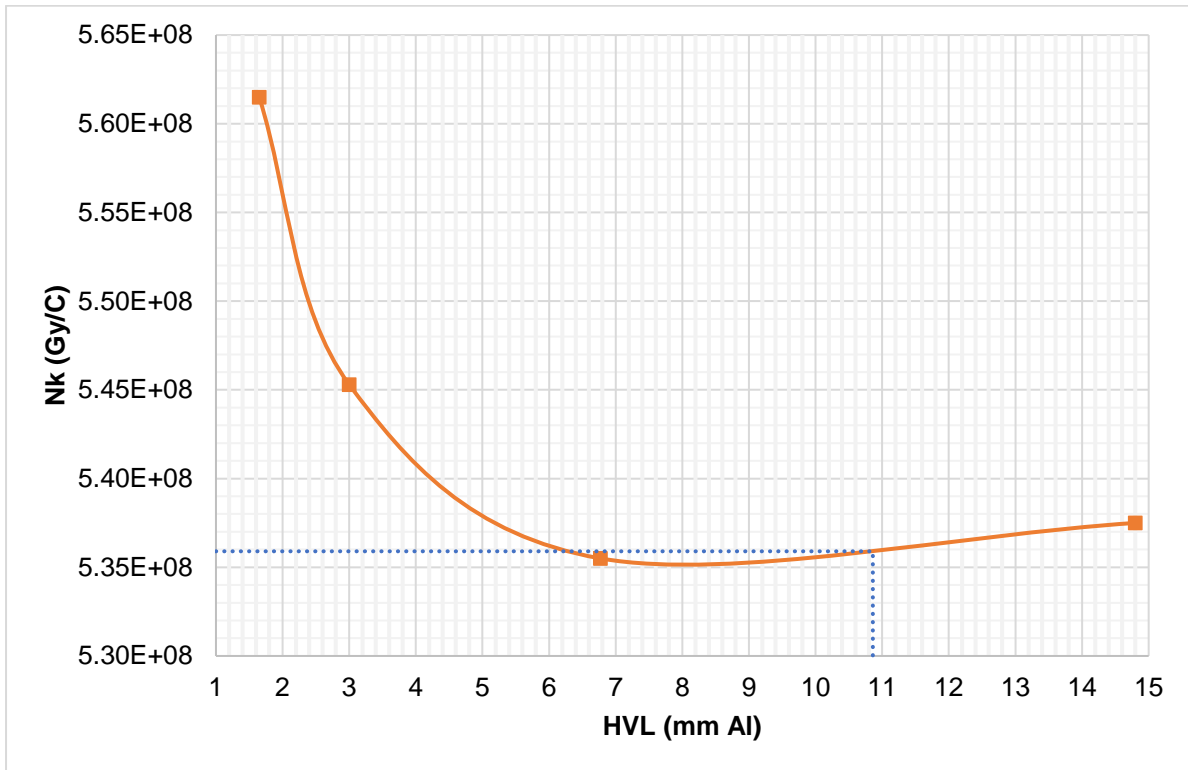
Figure 12. Plot of air-kerma calibration factor (N_K) versus half-value layer (HVL)

The TG-61 in-air method formula (Equation 2) was used to calculate absorbed dose to water at the surface of a water phantom ($D_{w,z=0}$):

$$\text{Equation 2: } D_{w,z=0} = M N_K B_w P_{stem,air} \left[\left(\overline{\frac{\mu_{en}}{\rho}} \right)^w_{air} \right]_{air}$$

where M is the ion chamber reading (corrected for ion collection efficiency, polarity, temperature and pressure, and electrometer accuracy) at the isocenter, N_K is the air-kerma calibration factor for the unit's beam quality (shown in Figure 12), B_w is the water phantom backscatter factor (TG-61, Table V), $P_{stem,air}$ is the chamber stem

correction factor, and $\left[\left(\frac{\overline{\mu_{en}}}{\rho}\right)^w_{air}\right]_{air}$ is the mean mass energy-absorption coefficient

ratio for water-to-air averaged over the incident photon spectrum (TG-61, Table IV)

(Ma, 2001). The experimental setup for TG-61 in-air measurements is shown in

Figure 13. The ion chamber was suspended in air at the isocenter with an in-house

plastic holder that attaches to the collimator. Measurements (60 seconds) were

taken in a field size of 10 cm x 10 cm, using 225 kVp tube potential, 13 mA current,

5 mm focal spot size, and 0.3 mm copper treatment filter.

Figure 13. Photograph of experimental setup for Task Group 61 in-air calibration

Determining Dose in the Mouse Phantom

As detailed in the section above, the TG-61 in-air calibration protocol determines the absorbed dose to the surface of a water phanto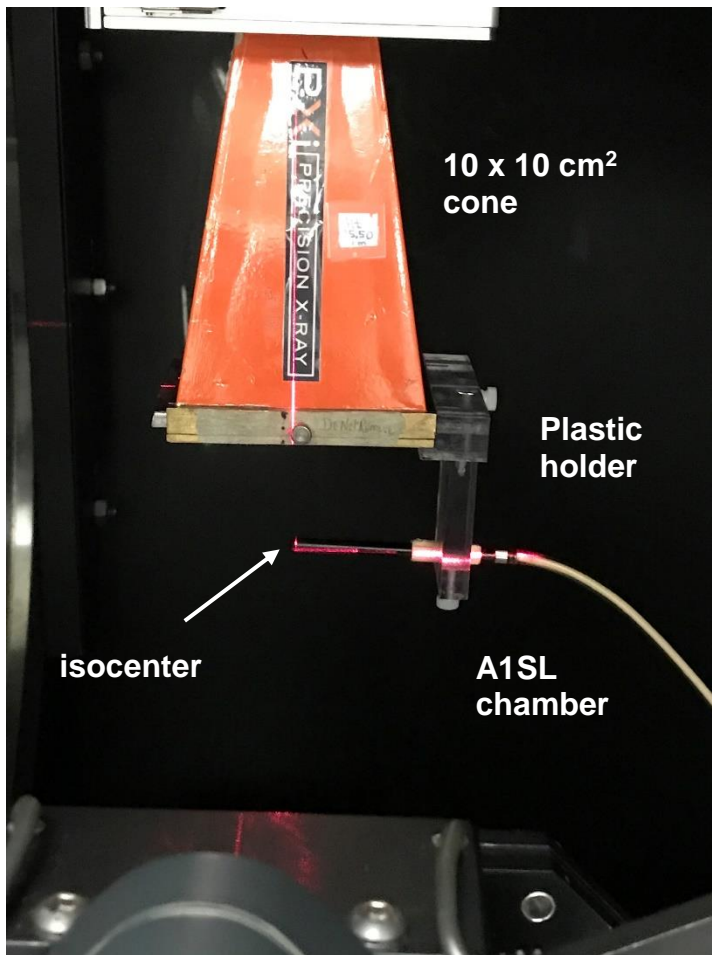m. However, of particular interest in developing independent peer review for small animal irradiators is the absorbed dose in a mouse phantom. The RDS defines the TLD reader sensitivity factor using TLD standards irradiated in a mini-phantom in a Co-60 beam to a known dose to muscle. Therefore, the dose to muscle at the location of the TLD in the mouse phantom was needed to commission the TLD for our independent peer review.

The air-kerma at the isocenter was calculated by rearranging equation 1 as the product of the corrected ion chamber reading at the isocenter and the air-kerma calibration factor for the X-RAD 225Cx beam quality. Because the ion chamber walls are thick enough to provide charged particle equilibrium in the orthovoltage energy range, the air-kerma is equivalent to the dose to air (Khan & Gibbons, 2014). Equation 3 was used to calculate dose to air at the isocenter.

$$\text{Equation 3: } D_{air}(Gy) = M_{corr}(C) * N_K\left(\frac{Gy}{C}\right)$$

The definition of "dose in free space" was then used to convert dose to air to dose to an equilibrium mass of water (Khan & Gibbons, 2014), shown in Equation 4 below.

$$\text{Equation 4: } D_{water,fs} = D_{air} * \left[\left(\frac{u_{en}}{\rho}\right)^w_{air}\right]_{air}$$

Because dose to muscle is of interest, dose in free space to water was converted to dose in free space to muscle using Equation 5 below:

$$\text{Equation 5: } D_{striated\ muscle,\ fs} = D_{water,fs} * \left(\frac{u_{en}}{\rho}\right)^{striated\ muscle}_{water}$$

where $\left(\frac{u_{en}}{\rho}\right)_{water}^{striated\ muscle}$ is the free-in-air ratio of the mass energy-absorption

coefficient of International Commission on Radiation Units and Measurements

(ICRU) striated muscle to water; these coefficients are listed in TG-61 (Table X) for

different biological tissues as a function of HVL. Finally, to convert from the dose in

free space to the dose in the mouse phantom, a "pseudo" tissue-air ratio (TAR) was

used. The TAR accounts for attenuation and scattering of the beam in the phantom.

It is defined as the ratio of the dose at a depth in a phantom (D_d) to the dose in free

space (D_{fs}) at the same point, Equation 6 (Khan & Gibbons, 2014).

$$Equation\ 6: TAR = \frac{D_d}{D_{fs}}$$

The TAR was determined by taking the ratio of the ion chamber reading in the ion

chamber mouse phantom (Figure 14a) to the reading in-air (Figure 14b) at the

isocenter. It should be noted that TAR is typically quoted for a specified field size,

as the phantom was larger than the radiation field. However, in this case, the mouse

phantom is smaller than the radiation field size. Therefore, TAR was defined as the

ratio of the reading in the ion chamber mouse phantom for a field of 8.5 cm by 2 cm

to the reading in-air for a field of 10 cm by 10 cm measured at the isocenter. Once

the TAR was determined, the dose to muscle at the center of the mouse phantom

was determined by taking the product of the dose to muscle in free space and the

TAR, as shown in Equation 7.

$$Equation\ 7: D_{striated\ muscle,mouse} = D_{striated\ muscle,fs} * TAR$$

The doses above were converted to dose rates by taking the ratio of the dose to the

irradiation time, accounting for timer error. The mouse phantom dose rate was then

used to determine the irradiation time needed to deliver a specified dose to muscle

of 300 cGy at the location of the TLD. The TLD mouse phantom was loaded with three TLD, placed on the irradiation stand, and aligned to the unit's lasers, shown in Figure 15. The irradiation time was selected on the animal irradiator console and the phantom was irradiated.
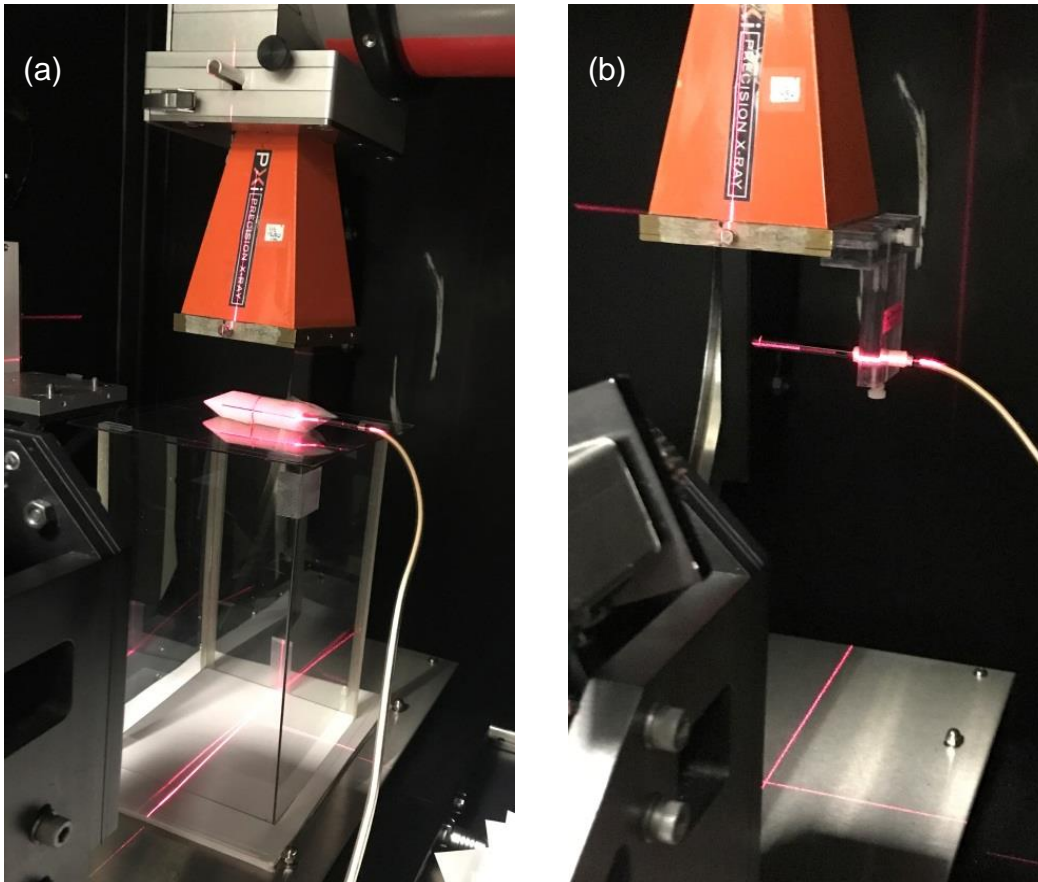
Figure 14. Experimental set-up for tissue-air ratio measurements
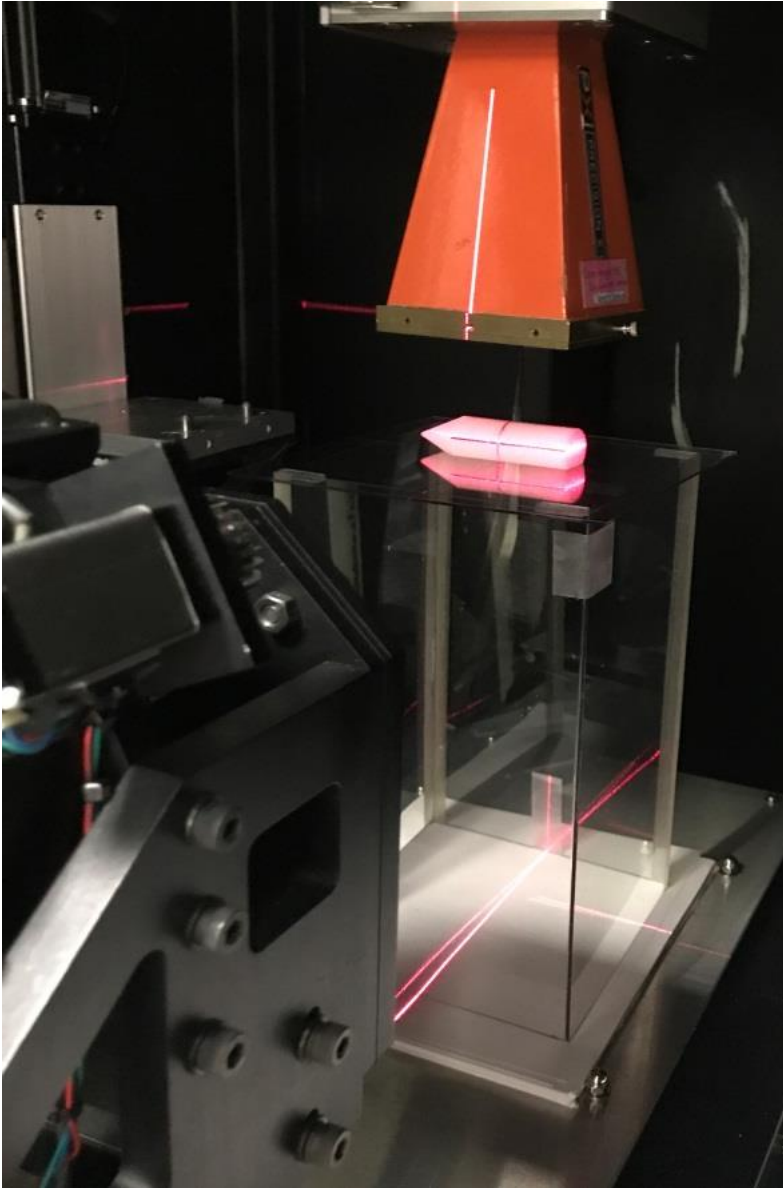
Figure 15. Experimental setup for delivering a known dose to the

thermoluminescent dosimeters in the mouse phantom

Results

Small Animal Irradiator Beam Output

Figure 16 is a plot of the half-value layer measured with copper attenuating

sheets for each measurement date. The average narrow-beam half-value layer

expressed in copper was 0.857 ± 0.002 mm Cu. Figure 17 is the corresponding plot

for aluminum attenuating sheets. The average narrow-beam half-value layer

expressed in aluminum was 10.86 ± 0.09 mm Al.
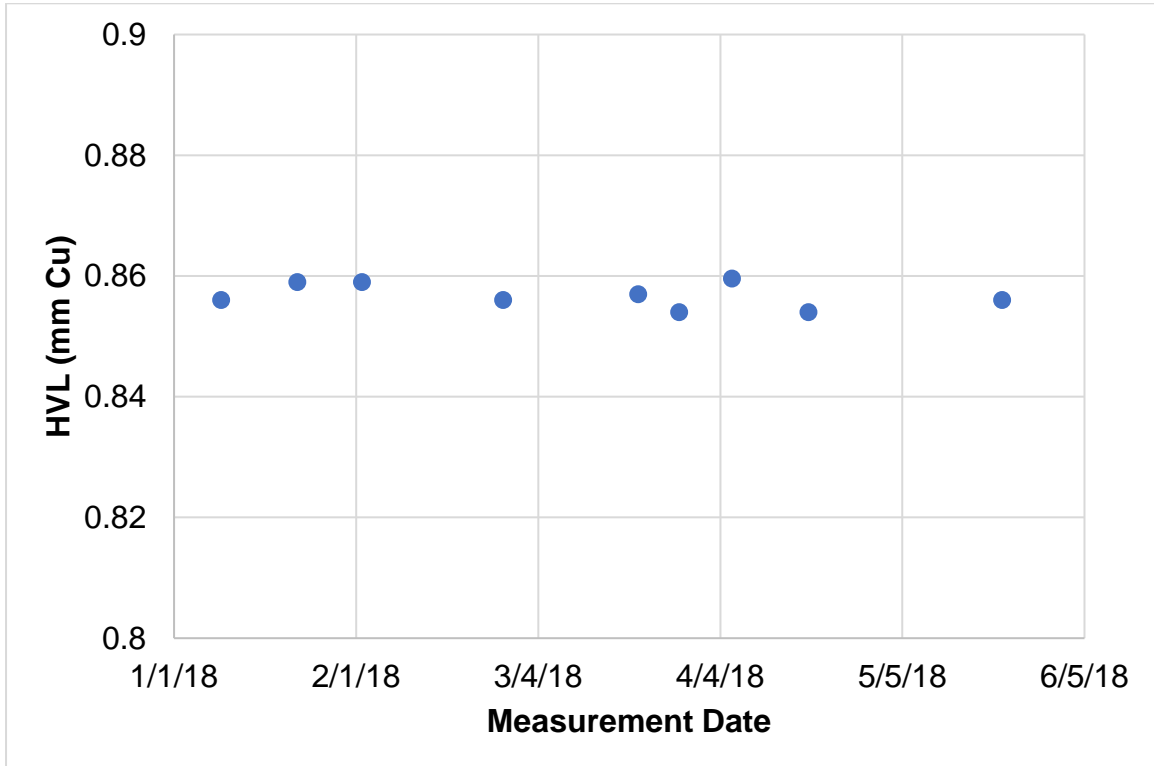
Figure 16. Results from narrow beam half-value layer measurements with copper

attenuating sheets
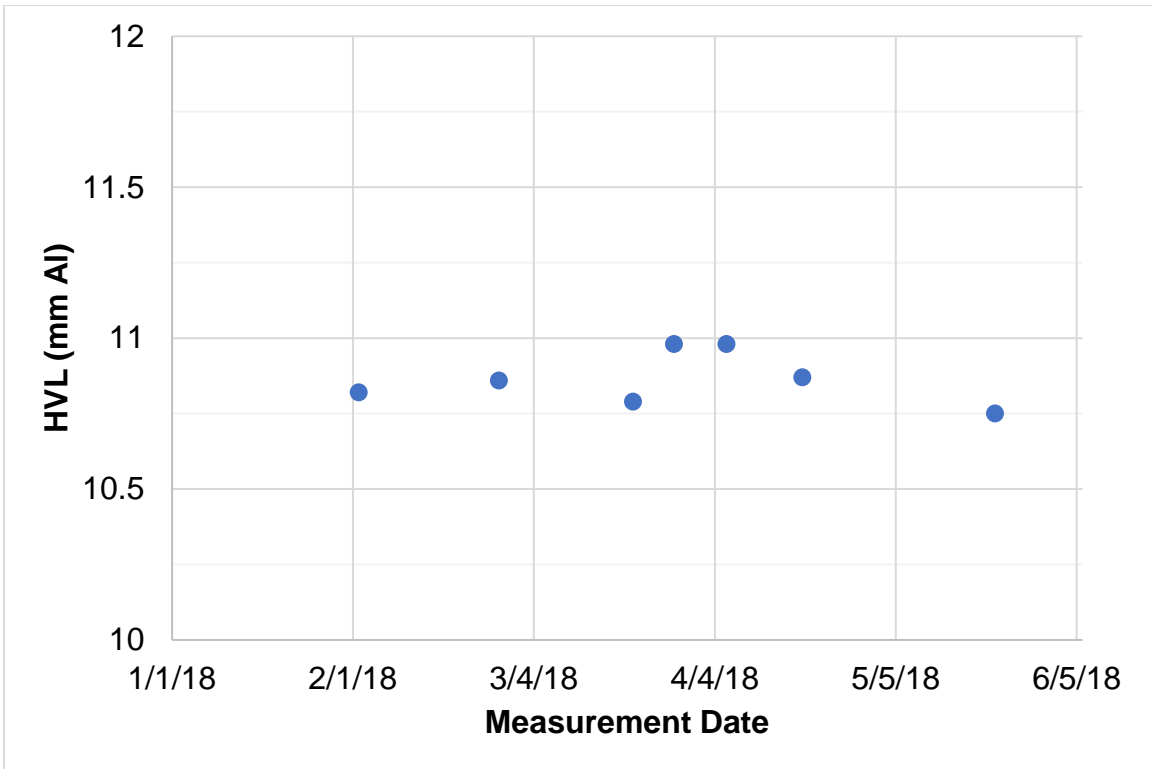
Figure 17. Results from narrow beam half-value layer measurements with aluminum attenuating sheets

Figure 18 is a plot of the TG-61 output, i.e., dose rate of absorbed dose to water at the surface of a water phantom, measured on different dates. The average output over a four-month time interval was 426.1 $\pm$ 3.9 cGy/min.
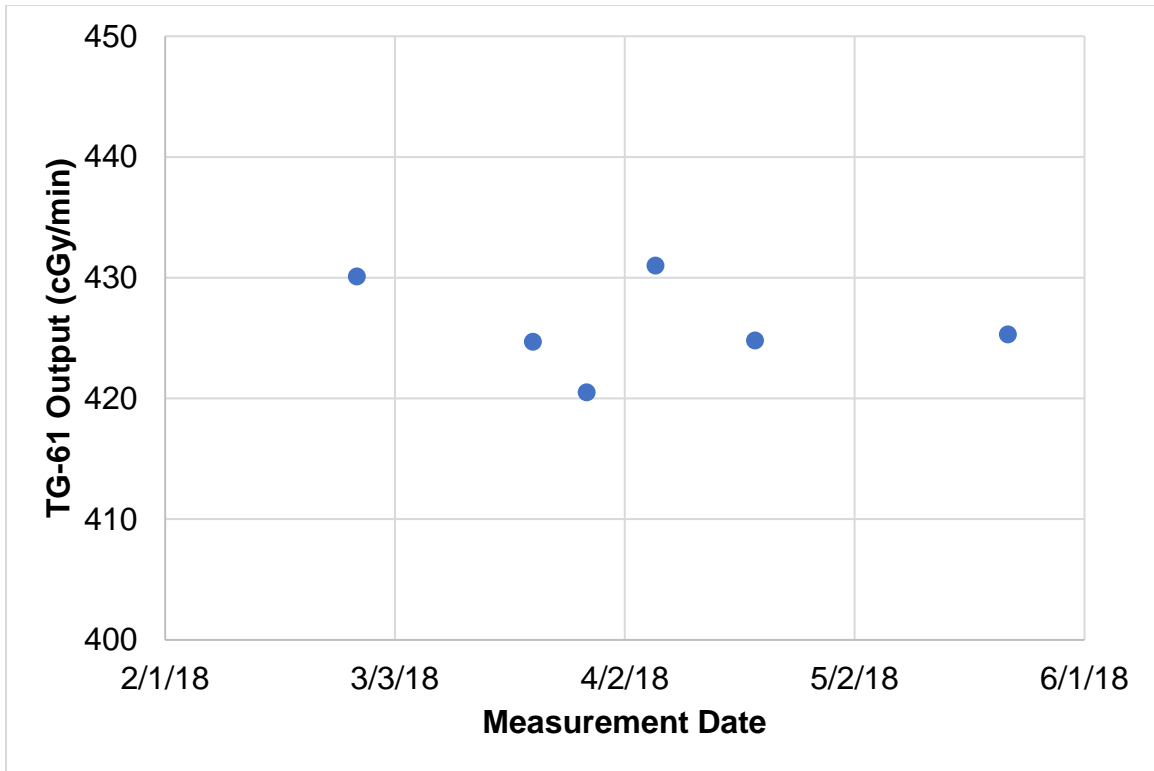
Figure 18. Task Group 61 orthovoltage beam output results

Dose rate in the mouse phantom

The average TAR was 1.075 ± 0.01. Figure 19 is a plot of calculated dose rate in the mouse phantom measured on different dates. The dose rate is reported in dose to muscle. The average dose rate over a four-month time interval was 341.2 ± 1.2 cGy/min.
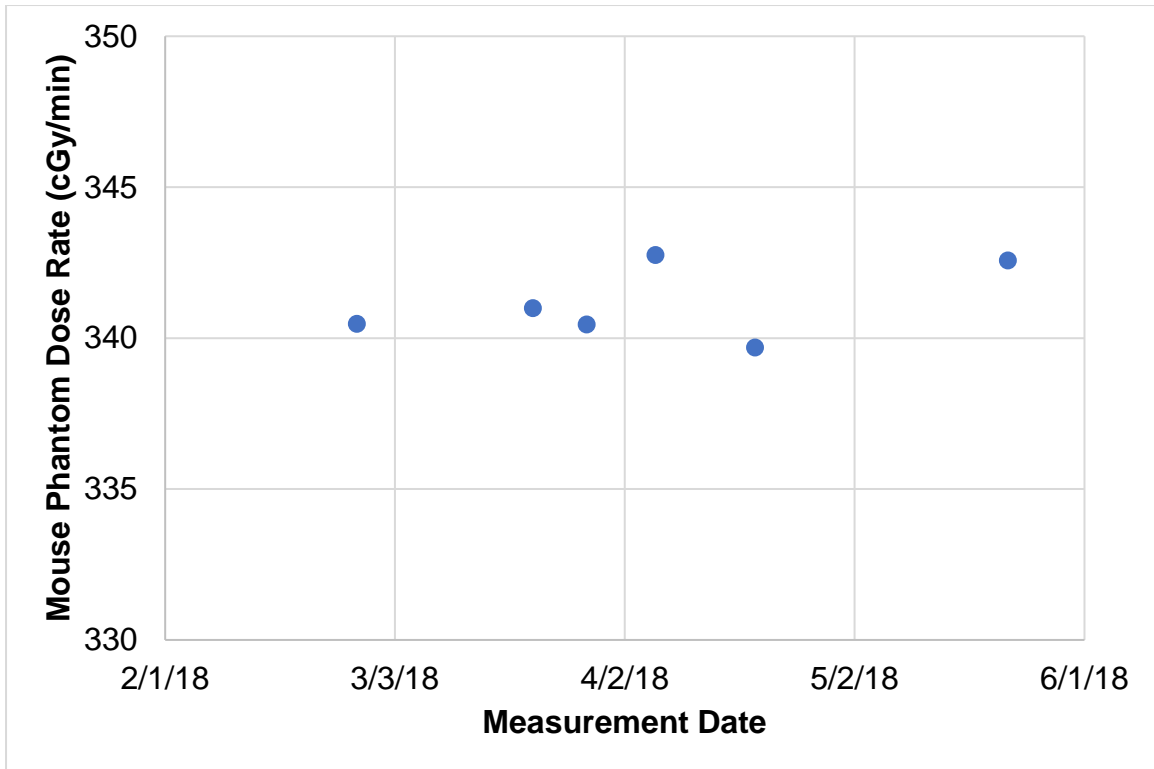
Figure 19. Measured dose rate in the mouse phantom

Characterizing the TLD Energy Correction Factor

Methods

Method 1: Comparison of Ion Chamber Dose to TLD Dose in Small Animal Irradiator

The first method that we used to determine the TLD energy correction factor in the mouse phantom was to compare the ion chamber dose to the TLD dose in the mouse phantom. The dose rate in the mouse phantom was determined by taking ion chamber measurements in the mouse phantom, as detailed above. A known dose was delivered to TLD in the mouse phantom. The TLD were read at RDS using a well-established independent beam output service, Radiation Dosimetry Services (Houston, TX), with an uncertainty of less than 1.5% (Kirby, T.H., Hanson,

W.F., Johnston, 1992). The energy correction factor, k_Q, was calculated (Equation 8) by setting the ion chamber dose equal to the TLD dose, as shown below:

$$D_{TLD} = M_{corr}Nk_Fk_Lk_Qk_\theta$$

$$D_{ion\ chamber} = D_{TLD}$$

Equation 8: $k_Q = \frac{D_{ion\ chamber}}{M_{corr}Nk_Fk_Lk_\theta}$

where M_{corr} is the corrected reading collected during the TLD readout process, N is the system calibration coefficient defined at a reference energy in Co-60, k_F is the fading correction factor, k_L is the linearity correction factor, and k_θ is the angular correction factor.

Method 1 was performed a total of 18 times over 5 different dates. At the outset of each performance, the dose rate in the mouse phantom was determined by ion chamber measurements. After the dose rate was determined, the mouse phantom was loaded with three TLD and irradiated to a known dose. Three irradiations were performed for each date, with the exception of six irradiations on March 28, when method 2 was conducted. The TLD energy correction factor was calculated for each irradiation.

Method 2: Comparison of TLD Signal from Small Animal Irradiator to Reference Co-60

The second method that we used to calculate the energy correction factor utilized the inherent definition of the energy correction factor: the ratio of the dose per reading from irradiation at a given energy to the dose per reading from irradiation at a reference energy, as represented in Equation 9 (Kry et al., n.d.):

$$\text{Equation 9: } k_Q = \frac{D_{exp}}{M(Q)_{exp}} \Bigg/ \frac{D_{ref}}{M(Q)_{ref}}.$$

The second method for determining the energy correction factor was to compare the signal from TLD irradiated in the mouse phantom in a reference Co-60 beam to the signal from TLD irradiated in the mouse phantom in the small animal irradiator.

The TLD irradiations in the mouse phantom in Co-60 and the small animal irradiator were performed on the same day. The TLD from both irradiations were read in the same reading session a week later to control for fading and sensitivity.

The procedure for delivering a known dose to TLD in the mouse phantom in the small animal irradiator is described in the section above. The procedure for delivering a known dose to the TLD in the mouse phantom in Co-60 is detailed below. First, the TG-51 calibration protocol was followed to calibrate the dose rate of the Co-60 unit (Almond et al., 1999). Measurements were taken in a 30x30x30 cm^3 water tank at a depth of 10 cm with an 80 cm source to surface distance (SSD) with an Exradin Model A12 0.64 cc farmer type chamber (Standard Imaging, Middleton, WI) centered in a 10 x 10 cm^2 field size. The measurements taken at 10 cm depth in the water tank were converted to dose rate using the following equation from TG-51 (Almond et al., 1999):

$$\text{Equation 10: } D_w^Q = \frac{M k_Q N_{D,w}^{Co-60}}{t_{set} - t_{error}}$$

where D_w is the dose rate to water at the measurement point in water; M is the ion chamber reading corrected for incomplete ion collection efficiency, polarity effects, temperature and pressure, and the electrometer accuracy; $N_{D,w}^{Co-60}$ is the absorbed dose to water calibration factor for the ion chamber (determined at a standards

laboratory); k_Q is the beam quality factor, which is equal to one because the measurements are performed in the same energy that the calibration coefficient is defined in; t_{set} is the time set on the timer, and t_{error} is the timer error.

Once the calibration at 10cm depth was completed, we used the following procedure was followed to convert dose at 10 cm depth in a water phantom to dose at 1 cm depth in the mouse phantom. First, the dose rate at 1 cm in the water phantom ($D_{1\ cm}$) was determined using published Co-60 percent depth doses (PDD) for the appropriate SSD and field size (Aird et al., 1996):

$$\text{Equation 11: } D_{1\ cm} = \frac{D_w^Q * PDD_{1\ cm}}{PDD_{10\ cm}}.$$

Next, the dose rate in full phantom was related to the dose rate in the mouse phantom by taking measurements with the A1SL ion chamber at 1 cm in the water tank and at 1 cm in the mouse phantom. The ratio of these readings is the ratio of the backscatter factors, shown in Equation 12:

$$\text{Equation 12: } B_{ratio} = \frac{M_{mouse\ phantom}}{M_{water\ tank}}.$$

The dose rate in the mouse phantom was calculated by multiplying the dose rate at 1 cm in the water phantom by the backscatter ratio, represented by Equation 13:

$$\text{Equation 13: } D_{mouse\ phantom} = D_{1cm} * B_{ratio}$$

Once the dose rate in the mouse phantom was determined, the irradiation time needed to deliver a known dose of 300 cGy to the TLD was determined. It should be noted that the set time was the real time plus the measured end-effect. Once the time was set, the mouse phantom loaded with TLD was irradiated on top of the irradiation stand with 80 cm SSD to the top of the mouse phantom. Six irradiations were performed, unloading and loading the TLD between irradiations.

On the same date (March 28, 2018) as the mouse phantom irradiations in Co-60, irradiations in the X-RAD 225Cx were performed. Ion chamber measurements were taken to determine the dose rate in the mouse phantom. Then, a known dose was delivered to the TLD in the mouse phantom in the small animal irradiator. Six irradiations were performed.

The TLD irradiated in Co-60 and the TLD irradiated in the small animal irradiator were read in the same session. The energy correction factor for Method 2 was calculated for each irradiation using the following equation:

$$\text{Equation 14: } k_Q = \frac{\left(D_{mouse} / M_{corr}*k_F*k_L \right)_{XRAD}}{\left(D_{mouse} / M_{corr}*k_F*k_L \right)_{Co-60}}$$

where D_{mouse} is the measured dose to muscle to the mouse phantom in cGy/min. Therefore, the energy correction factor is the ratio of the dose per corrected TLD signal for 225 kVp compared to reference Co-60.

Results

The average TLD energy correction factor for each irradiation date is plotted in Figure 20. The error bars represent the standard deviation between irradiations for a given date. The average TLD energy correction factors derived from Methods 1 and 2 were 0.792 ± 0.006 and 0.791 ± 0.006, respectively. An unpaired t-test yielded a two-tailed P value of 0.8783, indicating that there is no statistically significant difference between the results from Methods 1 and 2. Therefore, the average energy correction factor of 0.792 can be used to verify dose delivered by users of the service.
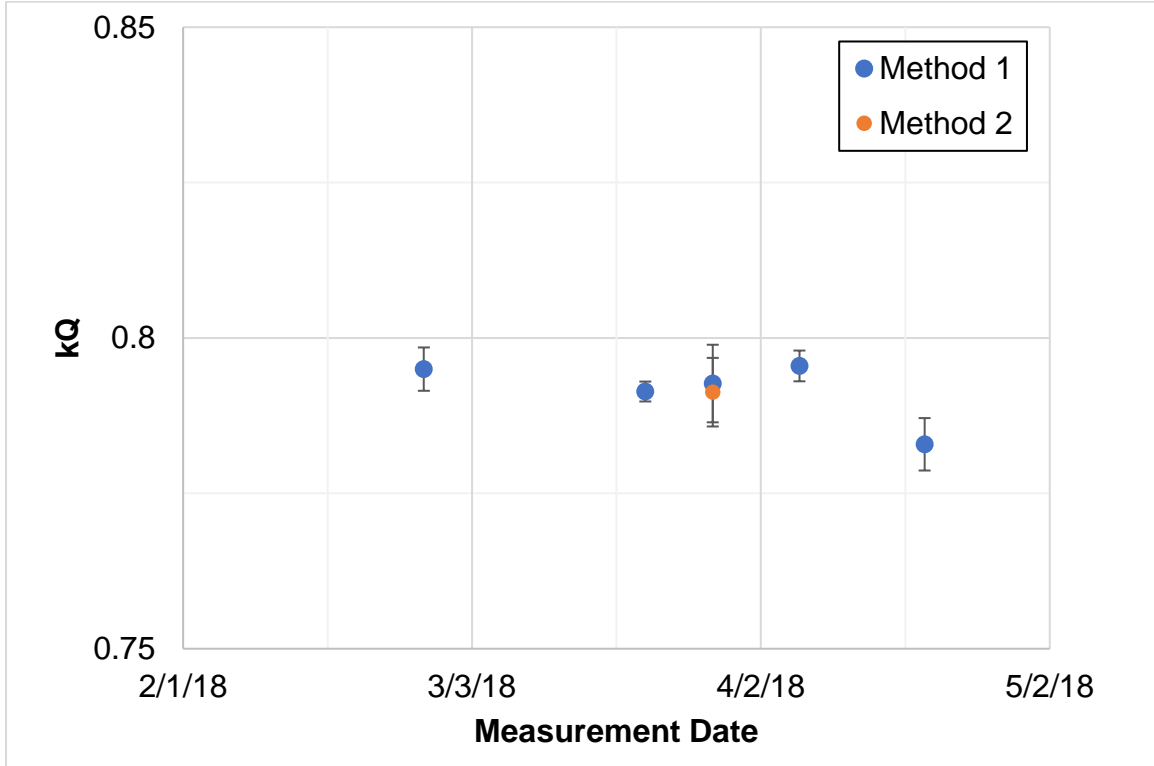
Figure 20. Comparison of Methods 1 and 2 for determining the energy correction

factor for thermoluminescent dosimeters in the mouse phantom

Statistical Analysis/Uncertainty in the Developed Independent Peer Review System

Methods

An uncertainty analysis in the TLD mail audit service was conducted

according to the methodology presented in Kirby 1992 (Kirby, T.H., Hanson, W.F.,

Johnston, 1992). This methodology computes the uncertainty in the determination

of dose using TLD by means of the TLD dose formula. It combines uncertainties in

measured TL signal, the system calibration factor, and each k-correction factor,

assuming that each is independent and normally distributed. The total uncertainty is

then determined by the quadrature sum of the individual uncertainties, as

represented in the equation below (Equation 4, Kirby 1992), and where a prime (') is
used to represent factors relating to TLD standards,

$$\text{Equation 15: } s_D^2 = \left(s_M \frac{\partial D}{\partial M}\right)^2 + \left(s_{D'} \frac{\partial D}{\partial D'}\right)^2 + \left(s_{k_Q} \frac{\partial D}{\partial k_Q}\right)^2 + \left(s_{M'} \frac{\partial D}{\partial M'}\right)^2 +$$

$$\left(s_{\left(\frac{k_F}{k_{F'}}\right)} \frac{\partial D}{\partial \left(\frac{k_F}{k_{F'}}\right)}\right)^2 + \left(s_{\left(\frac{k_L}{k_{L'}}\right)} \frac{\partial D}{\partial \left(\frac{k_L}{k_{L'}}\right)}\right)^2.$$

The uncertainty in the TLD energy correction factor, k_Q, was calculated by
combining our measurement uncertainty in the calculated value of k_Q and the
uncertainty in the measured ion chamber dose reported in TG-61 (Ma, 2001, Table
III). All other uncertainties in the TLD dose factors were taken directly from the work
of AAPM Task Group 91 (Kry et al., n.d., Table 6.2) . The total uncertainty in the
developed peer review service was then calculated using equation 15.

Results

The uncertainty in the developed mail audit service was determined (Table 4).
The resulting analysis indicated that the developed independent peer review service
has a 1-sigma uncertainty of 4.2%. However, this uncertainty is only applicable if
the HVL has been appropriately measured under narrow-beam geometry. The TLD
energy correction factor varies greatly with HVL in the orthovoltage energy range
(Kry et al., n.d.).

Variable	Uncertainty (%)
D_0	0.6
M_0	0.7
M_{raw}	1.7
k_L	0.1
k_F	0.7
k_θ	0.0
k_Q	3.7
Total (1-sigma)	**4.2**
Total (2-sigma)	**8.5**

Table 4. Uncertainty budget for the developed independent peer review system for the X-RAD 225Cx

Chapter 4: Conducting a Pilot Study

Measurements on another X-RAD 225Cx unit

Methods

In order to determine the variability in X-RAD 225Cx units and assess the feasibility of the independent peer review system, we collaborated with an X-RAD 225Cx user at another academic institution; hereafter, referred to as Institution A (for anonymity).

We were interested in comparing the beam output and mouse dosimetry measured in our irradiator to that of Institution A's irradiator. First, the narrow-beam HVL was determined and TG-61 output measurements were taken (following the previously described methods). Second, once the beam output was determined, ion chamber measurements in the mouse phantom were acquired to determine absolute dosimetry in the mouse phantom. Although MD Anderson and Institution A have identical irradiator models, the interior dimensions of the unit were not the same. The distance from the metal platform at the bottom of the irradiator to the isocenter is shorter by a couple centimeters in Institution A's irradiator. Therefore, the TAR experimental setup differed from that used at our unit because the irradiation stand was too tall to place the mouse phantom at the isocenter. The setup was modified by placing the mouse phantom on the animal platform and adjusting the stage to place the ion chamber at isocenter (Figure 21).
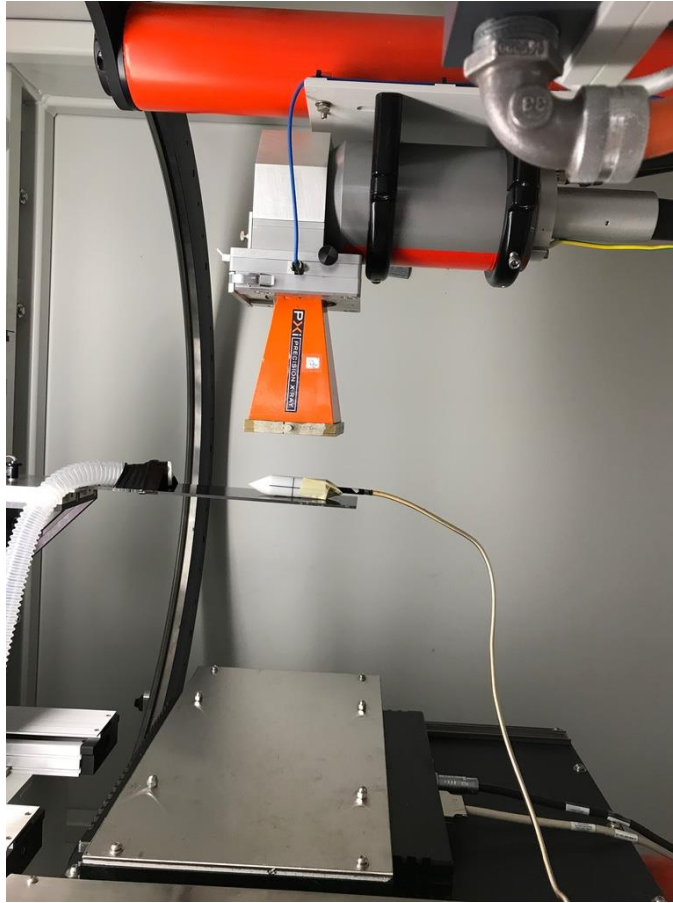
Figure 21. Experimental setup for pseudo tissue air ratio measurements in the mouse phantom at Institution A

Once the dosimetry in the mouse phantom was characterized with ion chamber measurements, TLD were irradiated to a known dose in the TLD mouse phantom according to Method 1 above in order to characterize the TLD energy correction factor. The TLD in the phantom were centered to the isocenter of the unit using the adjustable animal stage.

Results

Although the two animal irradiators are the same model, their beam qualities differed. This is likely the result of slight differences in the x-ray tube and filtration of

each unit. The measured beam quality of Institution A's irradiator was higher than that of our irradiator. The narrow-beam HVL of Institution A was 0.966 mm Cu and 11.49 mm Al; 12.9% and 5.4% (respectively) higher than our institution's HVL. The TG-61 output (absorbed dose to the surface of a water phantom) of Institution A was 370.0 cGy/min; 13.1% lower than our institution's average output. The pseudo TAR was 1.068, which is within the measurement range for our unit. As expected from the lower TG-61 output, the dose rate in the mouse was 13.5% lower, measuring 294.8 cGy/min to muscle.

Because the energy dependence of the ion chamber is negligible, there is no need for an ion chamber energy correction factor. This not the case for TLD dosimetry, where the sensitivity is dependent on the energy and particularly so in the orthovoltage energy range. The energy correction factor of the TLD in the mouse phantom was determined using Method 1. The average energy correction factor for Institution A was 0.811 ± 0.003. This energy correction factor is 2.4% higher than that of our institution (Figure 22). The higher correction factor means that the overresponse of TLD is lesser for Institution A; this is to be expected for higher beam qualities. Less of a correction is needed the closer the energy is to reference Co-60. The results of the feasibility measurements indicate the importance of properly characterizing the narrow-beam HVL for accurate TLD dosimetry.
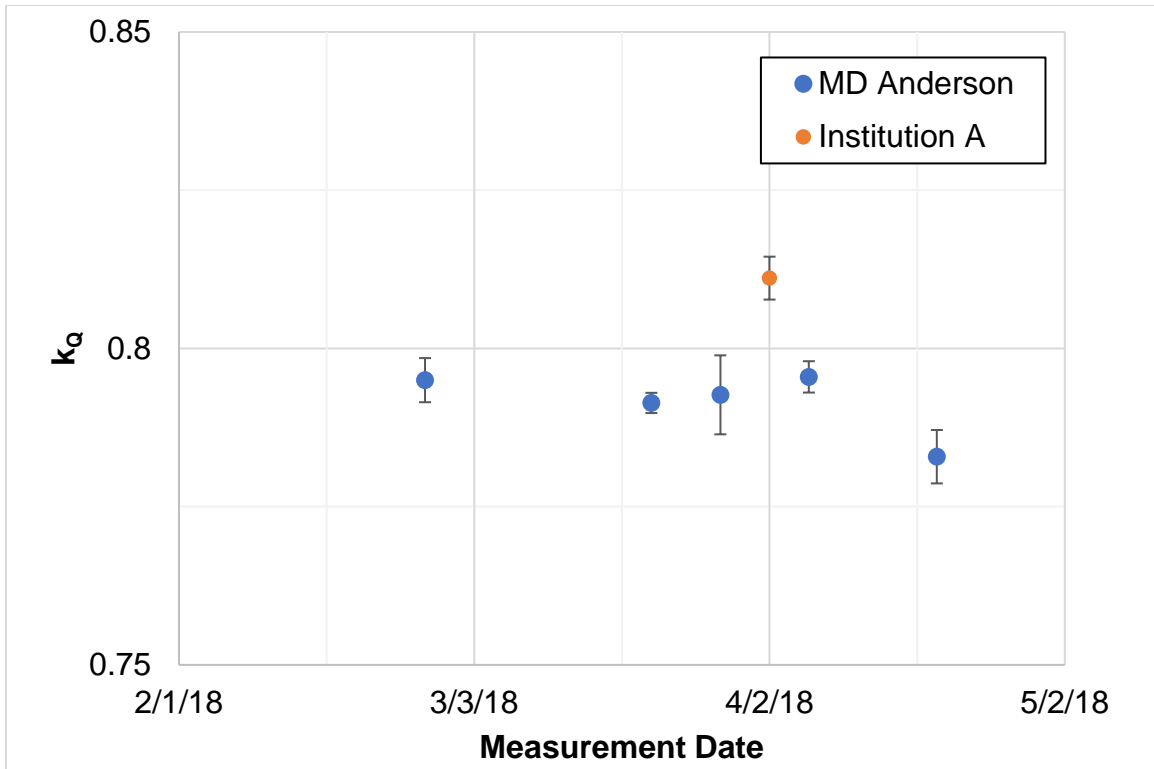
Figure 22. Comparison of thermoluminescent dosimeter energy correction factors

determined for X-RAD 225Cx animal irradiators at MD Anderson and Institution A

Mail Audit Feasibility Study

Methods

In order to test the feasibility of the developed mail audit service, we

conducted two test audits carried out at two different institutions. To each institution,

we sent the mouse phantom, irradiation stand, an irradiation data form (Figure 23),

and irradiation instructions (Figure 24). They were asked to deliver 300 cGy to the

center of the mouse phantom.

MONITORING OUTPUT OF AN ORTHOVLTAGE X-RAY BEAM FOR A SMALL ANIMAL IRRADIATOR

Institution: # _____ - _____ Date Mailed: _____

Date of Irradiation: _____

Person(s) Irradiating dosimeters: _____

Primary Physicist: _____

Physicist Email: _____ Phone Number: _____

Radiation Machine (manufacturer/model): _____ Serial Number: _____

kVp: _____ HVL: _____

Mouse Phantom Irradiation Conditions

Field size: _____ x _____ cm^2 OR _____ cm diameter circle

Timer setting: _____ sec

Timer/end error: _____ sec

Dose delivered: _____ cGy ◯ muscle

◯ soft tissue

◯ water

Backscatter factor: _____

Figure 23. Irradiation data form used for independent peer review feasibility studies

SMALL ANIMAL IRRADIATOR INDEPENDENT PEER REVIEW INSTRUCTIONS

INSTRUCTIONS FOR IRRADIATING TLD IN MOUSE PHANTOM

1. Assemble the irradiation stand as follows. Unfold the four legs into the shape of a rectangle and secure with a piece of tape. Place the platform top on the legs. The assembled stand is shown in the Figure 1.

Figure 1- Assembled irradiation stand and platform for mouse phantom

2. Place the assembled stand on the metal surface at the bottom of the irradiator. Place the mouse phantom loaded with TLD on top of the irradiation platform. Raise the height of the stand by adding paper underneath. Continue adding paper until the TLD are at the unit isocenter height, indicated by alignment of the horizontal side crosshair on the mouse with the horizontal laser (Figure 2). Once the height is correct, align the mouse phantom in all three dimensions. All crosshairs should coincide with the unit lasers (Figure 3).
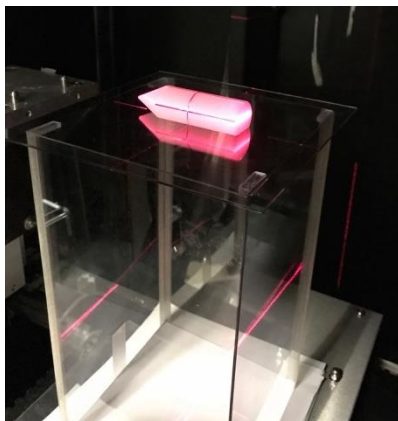

Figure 2- proper stand height has been reached, indicated by alignment of horizontal cross-hair with laser
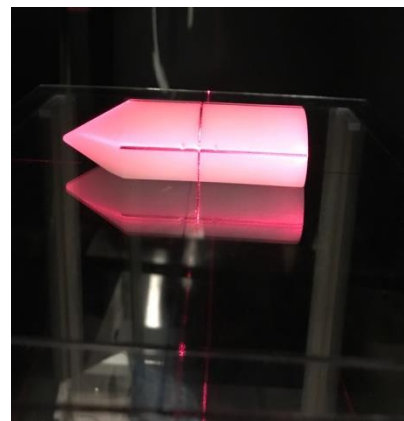
Figure 3- mouse phantom crosshairs aligned with irradiator lasers

55

3. Place the treatment filter and the 10 cm x 10 cm cone in the accessory tray. The complete irradiation setup is shown in Figure 4.
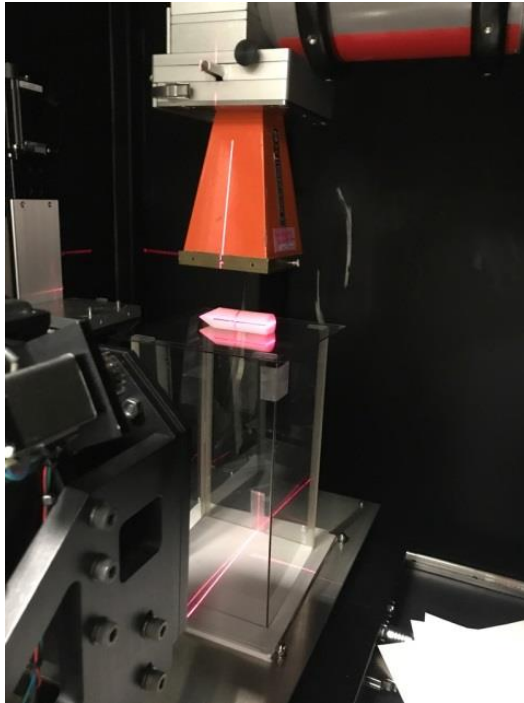
Figure 4- Setup for Mouse Phantom Irradiation

4. Set the irradiator to 225 kVp and 13 mA. Determine the irradiation time needed to deliver **300 cGy at 1 cm depth to the center of the mouse** at the isocenter for a 10 cm x 10 cm field size. Irradiate the phantom.

5. Complete the TLD datasheet. Fill in all requested information, as incomplete forms will delay the processing of your TLD. Please send back the TLD via regular U.S. mail using the address label provided. TLD cannot be read until 7 days after irradiation. **If you wish to return TLD by an express or direct carrier, use the following address: Radiation Dosimetry Services, 8060 El Rio Street, Houston, TX 77054.** If you have any questions, please call Radiation Dosimetry Services (RDS) at (713) 745-8999 or you may e-mail us at RDS@mdanderson.org.

Figure 24. Instruction form used for independent peer review for feasibility studies

Results

Mail Audit Results for Institution A

We selected institution A as one of the mail audit participants, since we had fully characterized their TLD dosimetry. The physicist responsible for the irradiator performed the mail audit. He specified that he delivered 300 cGy to water to the mouse with a backscatter factor of 1.35. The TLD were later read by RDS. Using our measured energy correction factor for institution A of 0.811, the calculated TLD dose was 224.9 cGy to water. The TLD dose was 25% lower than Institution A's specified dose of 300 cGy.

After follow-up with Institution A, we identified that they had treated the peer review output check as a TG-61 calibration check, rather than a mouse dosimetry check. Their irradiation time was selected based on the dose rate to the surface of a full water phantom, rather than the dose rate at 1 cm depth in a mouse. We converted Institution A's specified dose to the dose to the mouse phantom by accounting for the incorrect backscatter factor using Equation 16:

$$\text{Equation 16: } D_{mouse} = \frac{D_{full\,phantom}}{B_A} * TAR$$

where $D_{full\,phantom}$ is Institution A's specified dose of 300 cGy to water, B_A is institution A's specified backscatter factor of 1.35, and TAR is our measured backscatter in the mouse. D_{mouse} was calculated to be 238.9 cGy to water. Using an institution specified dose of 238.9 cGy, the calculated TLD dose was 229.6 cGy to water (using linearity correction factor based on D_{mouse}). The calculated TLD dose was 3.9% lower than D_{mouse}.

While this mail audit feasibility test demonstrated that Institution A has a properly calibrated unit, it did not answer the important question regarding whether the institution could deliver a specified dose to a mouse (or mouse phantom). Thus, we again followed-up with the physicist at Institution A and asked how he would determine the time needed to deliver 300 cGy to a mouse. He responded that an in-house Monte Carlo treatment planning software is used. Based on this feedback, we determined that a more appropriate test of small animal dosimetry would be an end-to-end test. For this type of test, we would instruct the user to image, treatment plan, and irradiate the phantom on the animal stage as they would a real mouse.

Mail Audit Results for Institution B

The mail audit was tested at a second institution, hereafter referred to as Institution B. A technician performed the irradiation at Institution B, rather than a medical physicist. Because some small animal irradiator users do not have physicists involved in the dosimetry, it is important that our audit procedures are easy to follow for both types of users. Based on the feedback from the mail audit with Institution A, we decided to have Institution B irradiate the mouse phantom as they would a real mouse, rather than following the original procedure (Figure 24). The institution imaged the phantom with on-board CBCT, developed a single-beam treatment plan to deliver 300 cGy to water at the location of the TLD capsules, and delivered the treatment. The TLD were later read by RDS, and it was determined that the TLD received a dose of 367.7 cGy to water, 22.6% higher than the specified dose. After contacting the institution and investigating the dosimetric discrepancy, it was determined that the dose rate that was used to irradiate the phantom was for an

incorrect field size, 10 mm x 10 mm rather than 10 cm x 10 cm. The institution was

asked to repeat the mail audit. The TLD measured dose from the repeat mail audit

was 309.7 cGy to water, 3.2% higher than the specified dose.

Chapter 5: Conclusions

General Review

We hypothesized that an independent peer review system for a small animal irradiator could be developed that has an uncertainty of less than ±10%. Specifically, that a mail audit service could be created with an action criterion of ±10%, meaning that mail audit users would be contacted by RDS technical staff if TLD discrepancies were outside of this criterion and a repeat irradiation would be suggested. This hypothesis was reasonable and perhaps overly permissive given that the experimental uncertainties in TLD dose measured using the RDS protocol are less than 1.5% (Kirby, T.H., Hanson, W.F., Johnston, 1992).

Our mail audit results indicated that two institutions were able to deliver a specified dose to the mouse phantom within ±5%, which is consistent with the 1-sigma uncertainty of 4.2% in the developed independent peer review service. However, it is important to note that the narrow-beam HVL was properly characterized by a physicist (with good narrow beam geometry) at both mail audit institutions. The TLD energy correction factor varies greatly with HVL in the orthovoltage energy range (Kry et al., n.d.). A comparison of measurements at MD Anderson and Institution A indicate that a difference in HVL as small as 0.1 mm Cu can result in a 2.5% difference in TLD energy correction factor. These differences can only be accounted for if the HVL is determined under narrow-beam geometry. However, many institutions do not measure HVL under narrow-beam geometry. In fact, many users do not measure HVL at all, but rather rely on manufacturer specifications (Seed et al., 2016). Therefore, while the output checks for the two

institutions evaluated in our feasibility study were within 5%, given the additional uncertainty in the HVL data from different institutions, a mail audit criterion of ±10% for the X-RAD 225Cx irradiator is more appropriate. Based on the measured variation in k_Q with HVL, a 1-sigma uncertainty of 10% is appropriate for beam qualities between 0.65 – 1.15 mm Cu HVL.

Future Work

The feasibility studies highlighted the importance of both beam output and end-to-end testing services for independent peer review. Moving forward, RDS will offer peer review services for both in-air output checks (preliminary results, Appendix B) and mouse phantom end-to-end dosimetric verification.

While TLD energy correction factors have been characterized versus HVL for clinical orthovoltage irradiators, further characterization is needed for cabinet irradiators. The narrow-beam HVL and TLD dosimetry both in-air and in-mouse phantom should be characterized for other X-RAD 225Cx irradiators in use.

This thesis work determined the TLD energy correction factor in the mouse phantom for a 10 cm x 10 cm field size. Future studies should be conducted to determine the variation of the TLD energy correction factor for different field sizes. While a 10 cm x 10 cm field size may be used for mouse total body irradiation, radiobiology studies typically use smaller field sizes to target localized regions of disease. Characterizing the TLD energy correction factor would allow researchers to test the dosimetry for their specific irradiation protocols.

Lastly, the methodology presented in this work should be expanded to other small animal irradiator models so RDS can provide more comprehensive service.

Given the apparent need for dosimetric standardization in small animal dosimetry and the lack of physics involvement, expanding the independent peer review service to include on-site visits for institutions with large dosimetric discrepancies will also be investigated.

Appendices

Appendix A: Effect of half-value layer geometry on TG-61 output

Methods

TG-61 requires accurate measurement of HVL under narrow-beam geometry. An in-house narrow-beam collimation device with a removable Cerrobend collimator (R Tailor) was used to determine the effect of narrow-beam collimation on TG-61 output. HVL measurements were taken with (Figure A-1a) and without (Figure A-1b) the narrow-beam collimator. The TG-61 in-air method was conducted to determine the effect of narrow-beam collimation on beam output.
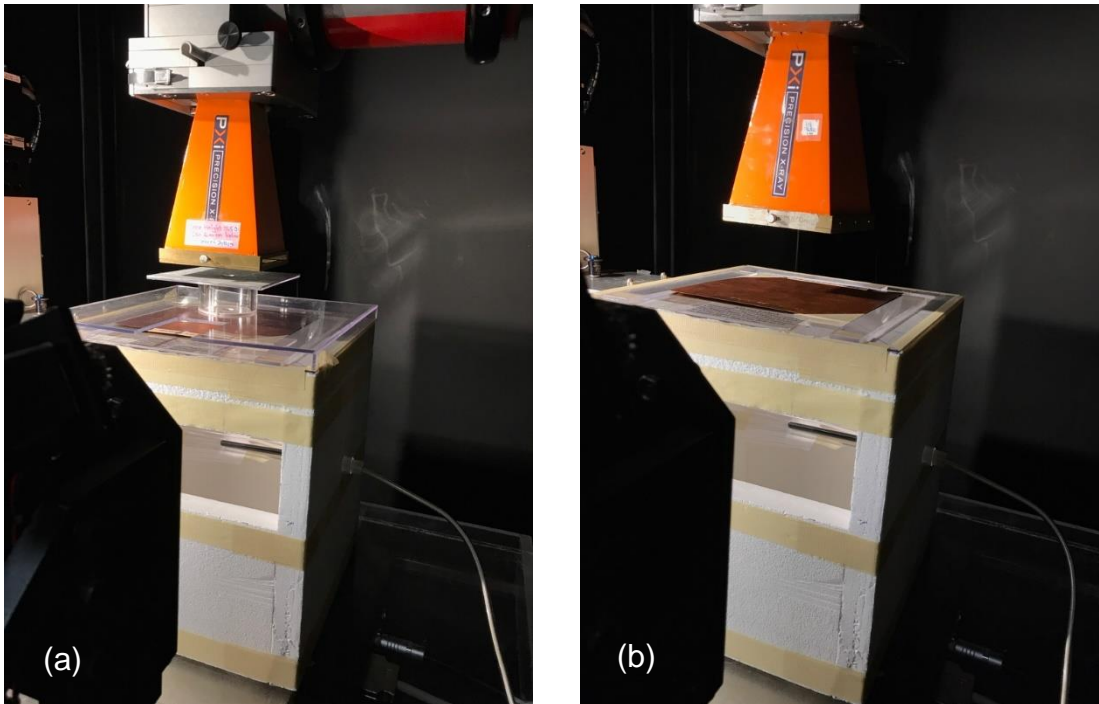

Figure A-1. (a) Experimental setup for measuring half-value layer under narrow-beam geometry, and (b) experimental setup for measuring half-value layer under good geometry

Results

The narrow-beam collimated HVL was determined to be 0.86 mm Cu and

10.82 mm Al. The half-value layer under good geometry, without narrow-beam

collimation, was determined to be 0.91 mm Cu and 12.97 mm Al. The 6%-20%

increase in half-value layer when the narrow-beam collimator is not used can be

attributed to an increase in scattered dose reaching the ion chamber. The TG-61

"in-air" method was used to determine absorbed dose to water at the surface of a

water phantom for each half-value layer result. An absorbed dose to water rate of

436.1 cGy/min and 435.5 cGy/min was determined for the narrow-beam geometry

and good geometry, respectively. These results are shown in Table A-1.

	With narrow-beam collimation	Without narrow-beam collimation
Copper HVL (mm Cu)	0.86	0.91
Aluminum (HVL)	10.82	12.97
TG-61 Output (cGy/min)	436.1	435.5

Table A-1. Impact of narrow-beam collimation on Task Group 61 output

Using our narrow-beam collimation device resulted in the most accurate dose

rate calculation for the X-RAD 225Cx small animal irradiator. However, using good

geometry without narrow-beam collimation proved to have a minimal impact (0.14%)

on the resulting calibrated output. Therefore, it can be concluded that making a

narrow-beam collimation device for HVL measurements of small animal irradiators is

not necessary for proper ion chamber dosimetry. However, properly characterizing

the HVL according to narrow-beam geometry is important for TLD dosimetry, as

there is a steep response between HVL and the TLD energy correction factor at orthovoltage energies.

Appendix B: Beam Output Check for small animal irradiators with In-Air TLD

Determining In-Air TLD Energy Correction Factor for X-RAD 225Cx

Methods

      RDS offers independent peer review of beam output for orthovoltage beams (typically for clinical units) with a passing criterion of $\pm$ 10%. The RDS has characterized the TLD energy correction factor in-air versus HVL measured in mm Cu (Figure B-1). The HVL expressed in copper was converted to aluminum using BJR 25 published data (Aird et al., 1996) (Figure B-2). The RDS has monitored beam output of the X-RAD 225Cx and X-RAD 320 small animal irradiators for three institutions over the last decade for HVL ranging from 0.9-1.035 mm Cu and 2.63-3.1 mm Al. A total of 20 mail audits between the three institutions has been performed. Every mail audit has passed the $\pm$ 10% criterion. The average ratio of TLD measured dose to institution stated dose was 0.979 $\pm$ 0.027. The average absolute percent difference was 2.8 $\pm$ 1.8%.
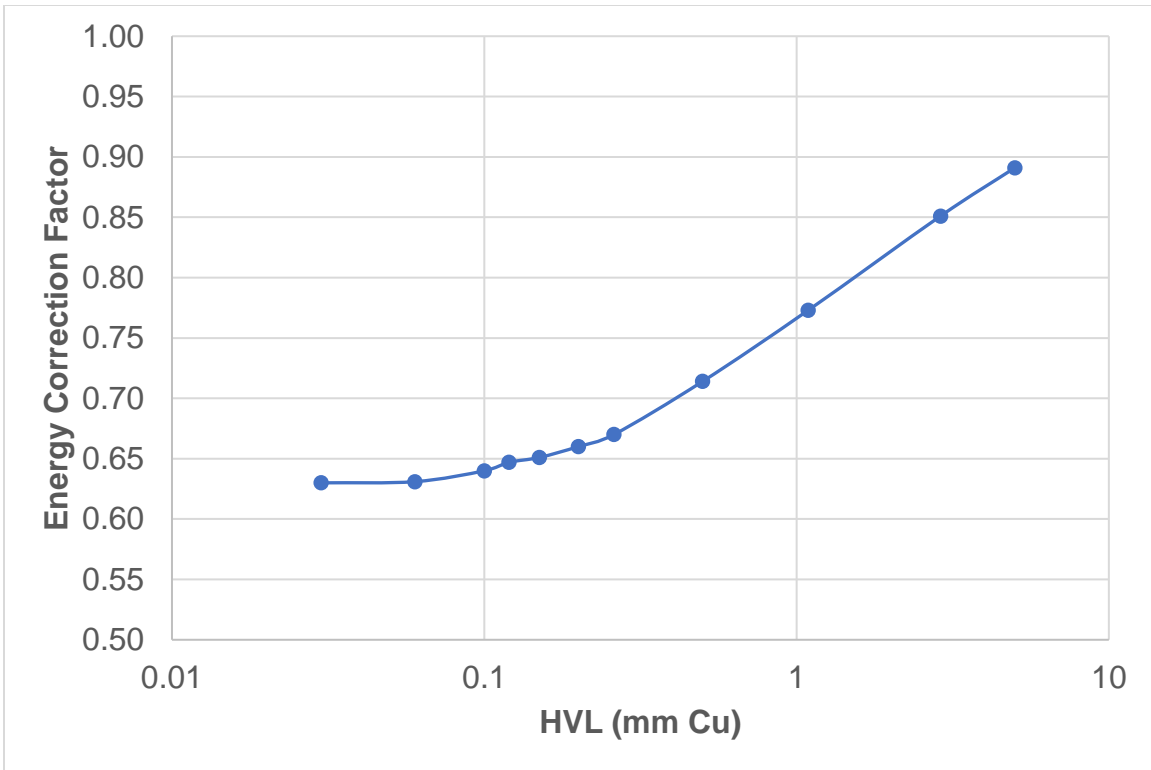
Figure B-1. Plot of RDS data for thermoluminescent dosimeter energy correction

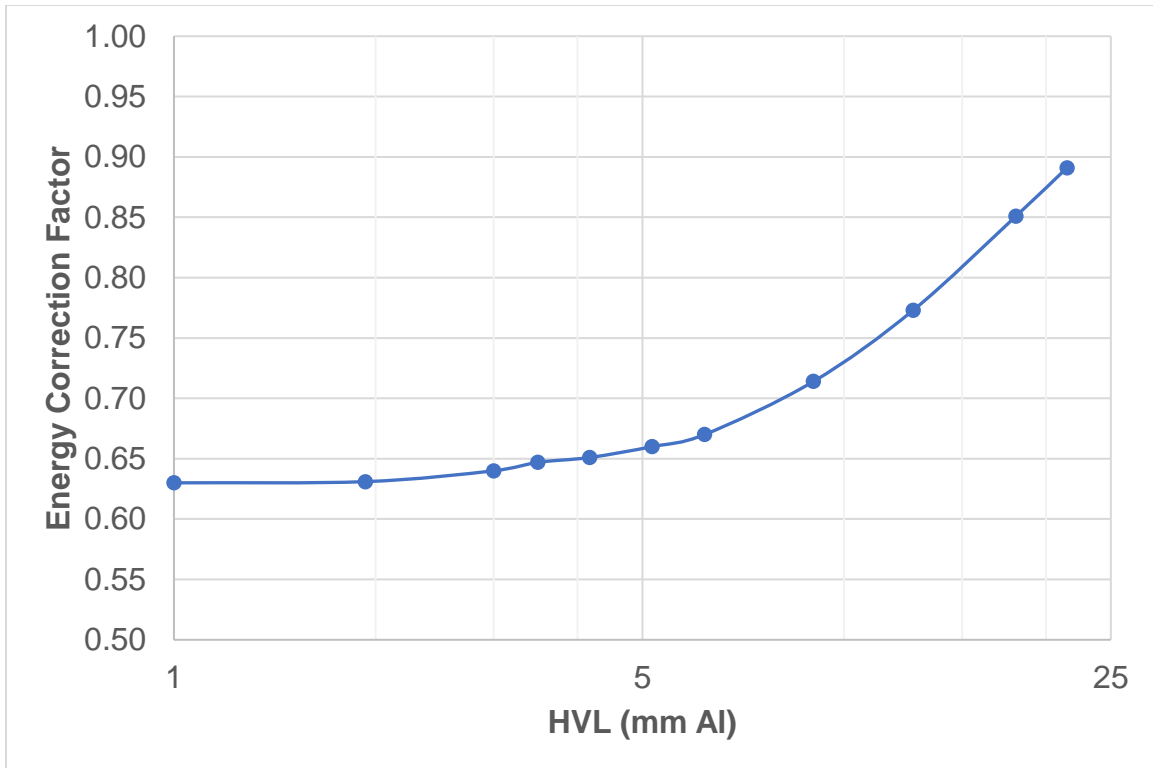factor versus half-value layer measured with copper attenuating sheets

Figure B-2. Plot of RDS data for thermoluminescent dosimeter energy correction factor versus half-value layer expressed in millimeters of aluminum

The TLD energy correction factor in-air in our X-RAD 225Cx unit and Institution A's unit was determined according to Method 1 presented in Chapter 3. TG-61 output measurements were converted to dose in free space to muscle. Measurements were taken with the A1SL chamber free in-air at the isocenter for a 10 cm x 10 cm field size, 225 kVp tube potential, and 13 mA tube current. Once the dose rate was determined with ion chamber measurements, TLD were suspended in-air from the irradiation stand using tape, aligned to the isocenter, and irradiated to a known dose (Figure B-3). The TLD were read, and the measured TLD dose was compared to the ion chamber dose to determine the TLD energy correction factor (Method 1).

Figure B-3. Experimental setup for irradiating thermoluminescent dosimeters in-air

Results

At MD Anderson, ion chamber measurements and TLD irradiations in-air were performed on five dates to characterize the TLD energy correction factor. The average dose rate in free space to muscle measuring with the ion chamber was 317.6 ± 3.2 cGy/min. The TLD energy correction factor was 0.797 ± 0.016. This is less than 1% different from the TLD energy correction factor in-mouse.

Institution A's TLD energy correction factor in-air was 0.831 ± 0.008. This is 2.5%

different from Institution A's correction factor in-mouse. The in-air TLD energy

correction factor data is shown in Figure B-4.

The TLD Energy correction factors for MD Anderson and Institution A were

compared to the values RDS uses for orthovoltage beam output. Based on Figure

B-1, MD Anderson's TLD energy correction factor should be 0.754 and Institution A's

should be 0.764. Therefore, using the RDS orthovoltage energy correction factor

data for the X-RAD 225Cx for MD Anderson and Institution A would result in

measured TLD errors of 5.4% and 8.0% respectively. These differences are likely

due to the differences in scatter environment of cabinet irradiators compared to

clinical orthovoltage irradiators. This result highlights the need to characterize the

TLD energy correction factor versus HVL for small animal irradiators.

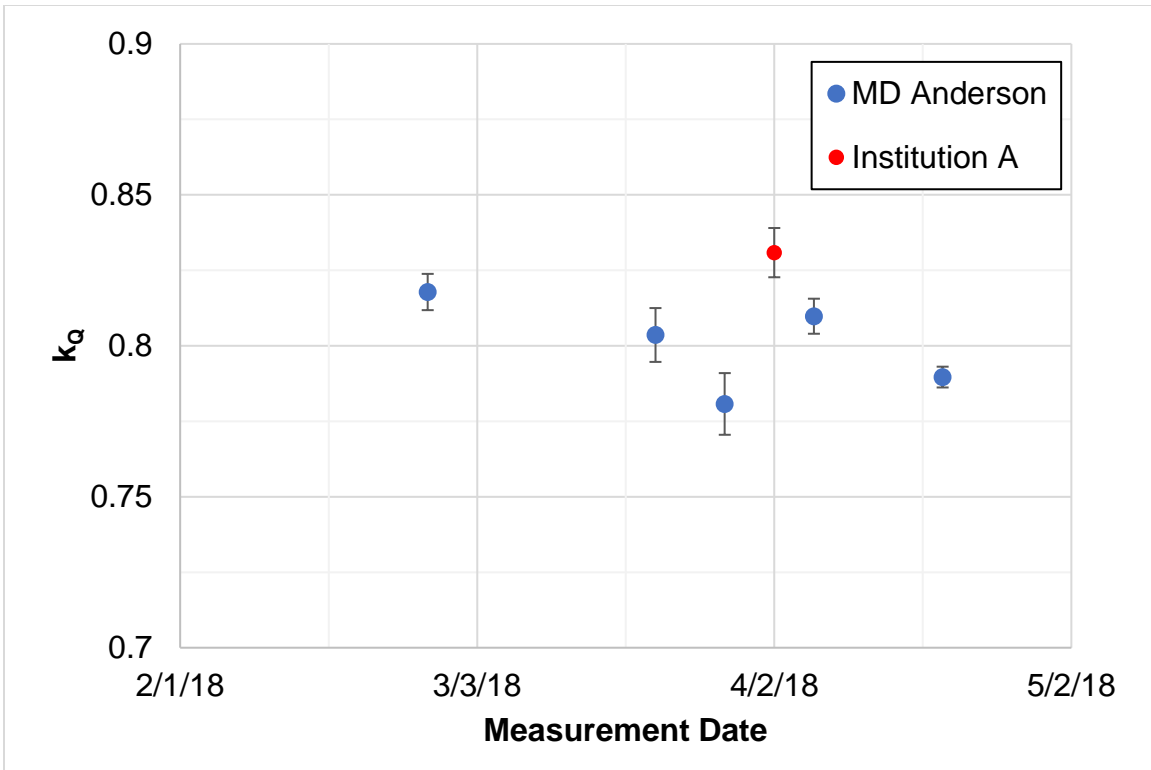**Figure B-4.** Thermoluminescent dosimeter energy correction factors in-air

Mail Audit Beam Output Checks for X-RAD 225Cx

Methods

Along with the in-mouse mail audit, Institutions A and B were asked to performing beam output checks with TLD suspended in-air. Figure B-5 contains the irradiation instructions for the output check. The institutions were asked to deliver 300 cGy in-air at their isocenter.

MONITORING OUTPUT OF ORTHOVOLTAGE BEAM FROM SMALL ANIMAL IRRADIATOR

INSTRUCTIONS FOR IRRADIATING TLD IN-AIR

1. Take the stand and the mouse phantom out of the irradiator. Remove the top platform on the irradiation stand, leaving just the legs of the stand. Place a long piece of tape across the top, as shown in Figure 1 below.   Make sure the tape is snug and doesn't sag.

Figure 1- Secure piece of tape
across the irradiation stand

2. Stick the three TLD capsules (colored plugs aligned in the same orientation) on a piece of tape and secure to the tape on the stand, as shown in Figure 2 below.

Figure 2- TLD capsules
secured to irradiation stand.

3. Place the stand inside the irradiator on the paper. Remove the 10 cm x 10 cm cone. Add more paper until the center of the TLD powder is aligned to the horizontal laser. Once you have reached the correct height, move the stand until the center of the TLD powder is at the isocenter, indicated by alignment with all of the lasers, shown in Figure 3 below.
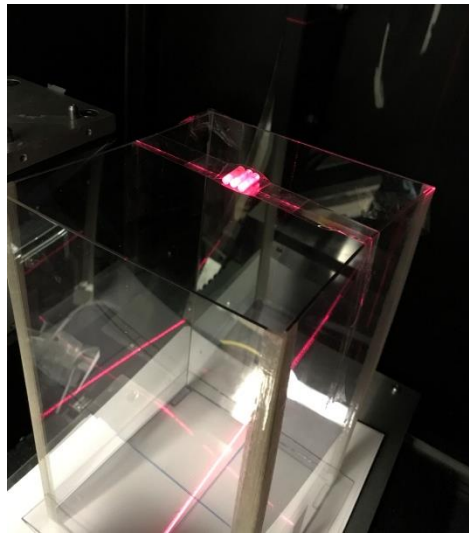

Figure 3- Aligning the TLD
powder to the unit isocenter

4. Insert the 10 cm by 10 cm cone. The irradiation setup is shown in Figure 4 below. Set the irradiation time to deliver a dose in free space of **300 cGy** at the location of the TLD.

Figure 4- Setup for in-air TLD irradiation

5. Complete the TLD datasheet. Fill in all requested information, as incomplete forms will delay the processing of your TLD. Please send back the TLD via regular U.S. mail using the address label provided. TLD cannot be read until 7 days after irradiation.
   If you wish to return TLD by an express or direct carrier, use the following address: Radiation Dosimetry Services, 8060 El Rio Street, Houston, TX 77054.
   If you have any questions, please call Radiation Dosimetry Services (RDS) at (713) 745-8999 or you may e-mail us at RDS@mdanderson.org.

Figure B-5. Beam Output Check Instructions

Results

       Both Institutions A and B stated that the TLD received 300 cGy to water. The

TLD measured dose for Institution A was 305.2 cGy to water; the ratio of measured

dose to institution stated dose was 1.02. The TLD measured dose for Institution B

was 299.5 cGy to water; the ratio of measured dose to institution stated dose was

0.99. Both institutions passed the beam output check well within the 10% criterion.

References

Aguirre, J. F., Tailor, R. C., Ibbott, G., Stovall, M., & Hanson, W. F. (2003).
Thermoluminescence dosimetry as a tool for the remote verification of output for
radiotherapy beams: 25 years of experience. *International Atomic Energy
Agency (IAEA)*, *2*, 191–199.

Aird, E. G. A., Burns, J. E., Day, M. J., Duane, S., Jordan, T. J., Kacperek, A.,
Klevenhagen, S. C., Harrison, R. M., Lillicrap, S. C., McKenzie, A. L., Pitchford,
W. G., Shaw, J. E., & Smith, C. W. (1996). BJR Supplement 25 Central Axis
Depth Dose Data for Use in Radiotherapy: 1996. *British Journal of Radiology*.

Almond, P. R., Biggs, P. J., & Hanson, W. F. (1999). AAPM ' s TG – 51 Protocol for
Clinical Reference Dosimetry of High-Energy Photon and Electron Beams b) a)
dose. *Medical Physics*, *26*(1999), 1–9.

Attix, F. H. (1986). *Introduction to Radiological Physics and Radiation Dosimetry*.
https://doi.org/10.1002/9783527617135

Butterworth, K. T., Prise, K. M., & Verhaegen, F. (2015). Small animal image-guided
radiotherapy: Status, considerations and potential for translational impact.
British Journal of Radiology, *88*(1045). https://doi.org/10.1259/bjr.20140634

Clark, C. H., Ga Aird, E., Bolton, S., Miles, E. A., Nisbet, A., Snaith, J. A., Thomas,
R. A., Venables, K., & Thwaites, D. I. (2015). Radiotherapy dosimetry audit:
Three decades of improving standards and accuracy in UK clinical practice and
trials. *British Journal of Radiology*, *88*(1055).
https://doi.org/10.1259/bjr.20150251

Craft, D. F., Kry, S. F., Balter, P., Salehpour, M., Woodward, W., & Howell, R. M.

(2018). Material Matters: Analysis of Density Uncertainty in 3D Printing and its

Consequences for Radiation Oncology. *Medical Physics*.

https://doi.org/10.1002/mp.12839

Desrosiers, M., Dewerd, L., Deye, J., Lindsay, P., Murphy, M. K., Mitch, M.,

Macchiarini, F., Stojadinovic, S., & Stone, H. (2013). The Importance of

Dosimetry Standardization in Radiobiology. *Journal of Research of the National

Institute of Standards and Technology*, *118*, 403–418.

https://doi.org/10.6028/jres.118.021

Hurkmans, C. W., Christiaens, M., Collette, S., & Weber, D. C. (2016). Beam Output

Audit results within the EORTC Radiation Oncology Group network. *Radiation

Oncology*, *11*(1), 1–6. https://doi.org/10.1186/s13014-016-0733-4

Ibbott, G. S. (2010). QA in radiation therapy: The RPC perspective. *Journal of

Physics: Conference Series*, *250*, 1–7. https://doi.org/10.1088/1742-

6596/250/1/012001

Izewska, J., Bera, P., & Vatnitsky, S. (2002). IAEA/WHO TLD Postal Dose Audit

Service and High Precision Measurements for Radiotherapy Level Dosimetry.

Radiation Protection Dosimetry, *101*(1–4), 387–392.

Khan, F., & Gibbons, J. (2014). *Khan's The Physics of Radiation Therapy*. (J. W.

Pine Jr, Ed.) (Fifth). Philadelphia: Lippincott Williams & Wilkins.

Kirby, T.H., Hanson, W.F., Johnston, D. A. (1992). Uncertainty analysis of absorbed

dose calculations from thermoluminescence dosimeters. *Medical Physics*,

19(6), 1427–1433. https://doi.org/10.1118/1.596797

Kry, S. F., Alvarez, P., Cygler, J., Dewerd, L. A., Howell, R. M., Meeks, S., O'Daniel,

J., Reft, C., Sawakuchi, G., Yukihara, E. G., & Mihailidis, D. (n.d.). *AAPM TG 191 Clinical Use of Luminescent Dosimeters: TLDs and OSLDs.*

Ma, C. -M., Coffey, C. W., DeWerd, L. A., Liu, C., Nath, R., Seltzer, S. M., Seuntjens, L. P. (2001). AAPM protocol for 40 – 300 kV x-ray beam dosimetry in radiotherapy and radiobiology, 868–893. https://doi.org/10.1118/1.1374247

National Institutes of Health, N. C. I. (2016). Cooperative Agreement to Develop Targeted Agents for Use with Systemic Agents Plus Radiotherapy (U01). Retrieved from https://grants.nih.gov/grants/guide/pa-files/PAR-16-111.html

Nunn, A. A., Davis, S. D., Micka, J. A., & DeWerd, L. A. (2008). LiF:Mg,Ti TLD response as a function of photon energy for moderately filtered x-ray spectra in the range of 20-250 kVp relative to60Co. *Medical Physics*, *35*(5), 1859–1869. https://doi.org/10.1118/1.2898137

Okamoto, H., Minemura, T., Nakamura, M., Mizuno, H., Tohyama, N., Nishio, T., Wakita, A., Nakamura, S., Nishioka, S., Iijima, K., Fujiyama, D., Itami, J., & Nishimura, Y. (2018). Establishment of postal audit system in intensity-modulated radiotherapy by radiophotoluminescent glass dosimeters and a radiochromic film. *Physica Medica*, *48*(18), 119–126. https://doi.org/10.1016/j.ejmp.2018.03.013

Pedersen, K. H., Kunugi, K. A., Hammer, C. G., Culberson, W. S., & DeWerd, L. A. (2016). Radiation Biology Irradiator Dose Verification Survey. *Radiation Research*, *185*(2), 163–168. https://doi.org/10.1667/RR14155.1

Radiation Dosimetry Services: Mailed Thermoluminescent Dosimeters (TLD) for Quality Assurance. (n.d.). Retrieved from

https://www.mdanderson.org/research/research-resources/core-

facilities/radiation-dosimetry-services.html

Radiation Monitoring by Mail Services. (n.d.). Retrieved from

https://uwmrrc.wisc.edu/?q=content/rmm-services

Sadikot, R. T. (2005). Bioluminescence Imaging. *Proceedings of the American

Thoracic Society*, *2*(6), 537–540. https://doi.org/10.1513/pats.200507-067DS

Scarboro, S. B., Followill, D. S., Howell, R. M., & Kry, S. F. (2011). Variations in

photon energy spectra of a 6 MV beam and their impact on TLD response.

Medical Physics, *38*(5), 2619–2628. https://doi.org/10.1118/1.3575419

Seed, T. M., Xiao, S., Manley, N., Nikolich-Zugich, J., Pugh, J., Van Den Brink, M.,

Hirabayashi, Y., Yasutomo, K., Iwama, A., Koyasu, S., Shterev, I., Sempowski,

G., Macchiarini, F., Nakachi, K., Kunugi, K. C., Hammer, C. G., & Dewerd, L. A.

(2016). An interlaboratory comparison of dosimetry for a multi-institutional

radiobiological research project: Observations, problems, solutions and lessons

learned. *International Journal of Radiation Biology*, *92*(2), 59–70.

https://doi.org/10.3109/09553002.2015.1106024

Small Animal Radiation Research Platform. (n.d.). Retrieved from

https://xstrahl.com/us/life-science-systems/small-animal-radiation-research-

platform/

Stone, H. B., Bernhard, E. J., Coleman, C. N., Deye, J., Capala, J., Mitchell, J. B., &

Brown, J. M. (2016). Preclinical data on efficacy of 10 drug-radiation

combinations: Evaluations, concerns, and recommendations. *Translational

Oncology*, *9*(1), 46–56. https://doi.org/10.1016/j.tranon.2016.01.002

Verhaegen, F., Granton, P., & Tryggestad, E. (2011). Small animal radiotherapy research platforms. *Physics in Medicine and Biology*, *56*(12). https://doi.org/10.1088/0031-9155/56/12/R01

Williams, I., Kenny, J., Lye, J., Lehmann, J., Dunn, L., & Kron, T. (2012). The Australian Clinical Dosimetry Service: A commentary on the first 18 months. *Australasian Physical and Engineering Sciences in Medicine*, *35*(4), 407–411. https://doi.org/10.1007/s13246-012-0161-1

X-RAD SmART Small Animal Image Guided Irradiation System. (n.d.). Retrieved from http://www.pxinc.com/products/small-animal-igrt-platform/x-rad-smart-small-animal-radiation-therapy-precision-xray-branford-connecticut/

Yegingil, Z., DeWerd, L. A., Davis, S. D., Hammer, C., & Kunugi, K. (2012). Photon beam audits for radiation therapy clinics: A pilot mailed dosemeter study in Turkey. *Radiation Protection Dosimetry*, *148*(2), 249–257. https://doi.org/10.1093/rpd/ncr017

Zakeri, K., Coleman, C. N., & Vikram, B. (2018). Radiation Oncology in the 21st Century : Prospective Randomized Trials That Changed Practice … or Didn ' t ! *Fronteriers in Oncology*, *8*(April), 1–10. https://doi.org/10.3389/fonc.2018.00130

Vita

Mary Elizabeth Peters was born in Atlanta, Georgia, the daughter of Patricia Lee Peters and Daniel Robert Peters. After completing high school at Alpharetta High School, Alpharetta, Georgia in 2012, she enrolled at the Georgia Institute of Technology in Atlanta, Georgia. She received the degree of Bachelor of Science with a major in Nuclear and Radiological Engineering from Georgia Tech in May 2016. In August of 2016, she entered the Medical Physics Program at The University of Texas MD Anderson Cancer Center UTHealth Graduate School of Biomedical Sciences.

Permanent address:

320 Kincardine Way

Alpharetta, GA 30022